# Development of Graphene Oxide based Ethylene Gas Sensor for Freshness Monitoring of Fruits

Thesis Submitted for the Degree of Doctor of

Philosophy (Science)

To

Jadavpur University

By

**Mintu Mallick**

[Index No: 57/15/Phys./23]

Under the Joint Supervision of

**Prof. Jayoti Das & Dr. Syed Minhaz Hossain**

Department of Physics
Jadavpur University
Kolkata- 700032, India
2023

***Dedicated***
***To***
***My Family***

# Certificate From the Supervisors

This is to certify that the thesis entitled "**Development of Graphene Oxide based Ethylene Gas Sensor for Freshness Monitoring of Fruits**" submitted by **Sri Mintu Mallick** who got his name registered on **28th April, 2015**. For award of **Ph.D. (Science)** degree of Jadavpur University, is absolutely based upon her own work under the joint supervision of **Prof. Jayoti Das** and **Dr. Syed Minhaz Hossain** and that neither this thesis nor any part of it has been submitted for either any degree/ diploma or any other academic award anywhere before.

Jayoti Das
23/02/2023
[Prof. Jayoti Das]
Signature of the Supervisor &
date with official seal

Dr. Jayoti Das
Professor
Department of Physics
Jadavpur University
Kolkata - 700 032

23/02/2023
[Dr. Syed Minhaz Hossain]
Signature of the Supervisor &
date with official seal

Dr. S. M. Hossain
Associate Professor & Head
Department Of Physics
Indian Institute Of Engineering Science & Technology, Shibpur
Howrah - 711103

# *LIST OF PUBLICATIONS*

1. **Mintu Mallick**, Deeparati Basu, Syed Minhaz Hossain, Jayoti Das, "Ethylene Sensor based on Graphene Oxide for Fruit Ripeness Sensing Application" Applied Physics A, 129:140, **2023**, DOI: https://doi.org/10.1007/s00339-023-06413-7.

2. Kaustuv Das, Bijoy Jana, Mousumi Pramanik, **Mintu Mallick**, Jayoti Das, Joydip Sengupta, "Chemically synthesize ZnO Nanocrystal-based ethylene sensor operative at natural humid condition", Applied Physics A 128:962, **2022**. DOI: https://doi.org/10.1007/s00339-022-06110-x.

3. **Mintu Mallick**, Syed Minhaz Hossian, Jayoti Das, "Graphene Oxide Based Fruit Ripeness Sensing e-Nose, Materials Today: Proceedings 5, **2018**, pp. 9866-9870. https://doi.org/10.1016/j.matpr.2017.10.179.

4. **Mintu Mallick**, Jayoti Das, "Graphene Oxide based ethylene gas sensor for e-nose application", Invertis Journal of Science and Technology, Vol.10, No. 4, **2017**, pp. 178-182. DOI: 10.5958/2454-762X.2017.00029.4.

5. **Mintu Mallick**, Mousumi Pramanik, Deeparati Basu, Purbasha Haldar, Kaustuv Das, Syed Minhaz Hossain, Anushka Banerjee, Dwaipayan Basu, Jayoti Das, Fruit Freshness Sensor based on Graphene Oxide, **2023**, (**Communicated to Silicon Journal**).

# *PREFACE*

In our daily life, fruits are very essential, but perfect ripe fruits are not so easy to identify by observing the change of colour in natural way, it turns into brown or blackish and futile very fast. In United States only, about 20% of all produced fruits and vegetables are lost due to spoilage in every year.

Unsaturated non-polar hydrocarbon, ethylene ($C_2H_4$) is a small plant hormone, regulates many developments process of plants. This gas is quite helpful to quickly ripen fruits and vegetables. The internal concentration of ethylene from fruits can indicate the proper time of harvest and detecting atmospheric ethylene level in a storage chamber we can avoid over ripening of fruits before transportation.

Ethylene gas concentration is now monitored via gas chromatography detection, electrochemical sensing or laser acoustic spectroscopy, all of these are very expensive and are not suitable for in-field measurement.

This thesis deals with the development of Graphene Oxide (GO) based Ethylene gas sensor for freshness monitoring of fruits. A conductive type GO-based pellet sensor and also drop casted thin film sensor have been fabricated and fruit ripeness condition is monitored via Ethylene gas sensing in a closed chamber at room temperature. Here we used fruits as the source of ethylene.

GO was prepared by standard Hummer's method, and morphological and structural characterizations have been performed using field emission scanning electron microscopy (FESEM), X-ray powder diffraction (XRD), and Raman spectroscopy analysis.

Four different types of fruits of same weight (200gm of orange, banana, guava, and mango) were used for sensor response measurements. Fruit samples were kept in the closed chamber, and the change in conductivity of the sensors (both pellet and thin film based) were observed with increase in emitted Ethylene concentration in the chamber which was cross-verified with standard MSR sensor. The sensors showed almost linear response in the Ethylene concentration range of 40–120 PPM, and it was observed that orange samples produce maximum response for the GO pellet sensor with a sensitivity of 0.06 μAmp/PPM for a fixed exposure time (5 minute). The sensor was found capable to successfully differentiate between four individual fruit samples in perfect ripening condition which could be utilized in fruit detector e-nose application.

From the response characteristics, different sensor parameters like, sensitivity, repeatability, reproducibility, storage stability have been studied. Studies on temperature optimization and humidity interference have also been performed. The studies show good response and an excellent repeatability. The storage stability of the sensors is also very good up to 10 days in ambient air. The optimized operating temperature of our sensors is found to be ~22°C, which is an added advantage for hydrocarbon gas sensing. Further, a comparative study between the response of our developed GO sensor and the sensors based on different well known gas sensing materials like ZnO and $MoS_2$ towards ethylene have been performed. All of these studies conclude that our GO based sensors can be a promising alternative for cost-efficient measurement of ethylene gas at room temperature.

The integration of the sensor with commercially available radio frequency identification device (RFID) tags for in-field wireless monitoring of the ripening condition of fruits may be the future scope of work.

# *ACKNOWLEDGEMENTS*

I want to express my gratitude to everyone who helped with the work that was the subject of this thesis. I want to start by expressing my gratitude to Pro. Jayoti Das (Department of Physics, Jadavpur University), who was my first academic supervisor. She gave me intellectual independence in my work during her tenure, supported my attendance at various conferences, exposed me to new ideas, and demanded a high standard of work in all my activities, all of which helped to make graduate school rewarding. She served as a second guardian in my work, without whom I could not have finished this thesis.

For his professional counsel and extensive resources, I am also very grateful to my second supervisor, Dr. Syed Minhaz Hossain (Department of Physics, IIEST Shibpur). I owe him a sincere debt of gratitude for all the assistance he provided in developing sensor setups and numerous other research areas, without which my work would not have been complete. His inspiration and direction have had a significant impact on me, which has allowed me to better appreciate the worth of fruitful research.

I would like to acknowledge Dr. Kaustuv Das (Department of Physics, Jadavpur University) for supporting and motivating me through this long period. I would also like to thank Prof. Sukhen Das (Department of Physics, Jadavpur University) for his immense technical support. A special thanks to Prof. Sanat Karmakar (Department of Physics, Jadavpur University) and Prof Sanjay Kumar (Department of Physics, Jadavpur University) who has provided technical support time to time. Also, am grateful to Prof. Partha Pratim Ray (Department of Physics,

Jadavpur University), Prof. Brajadulal Chattopadhya (Department of Physics, Jadavpur University) and Prof Chittyaranjan Sinha (Department of Chemistry, Jadavpur University), I wish to acknowledge my deepest respect towards him.

I would like to acknowledge Rajiv Gandhi National Fellowship, UGC, India, for providing fellowship throughout the tenure of my research. The financial support helped me immensely in uninterrupted research work.

I would like to thank my colleagues Deeparati, Tanusree di, Arnesh, Kaustav and Chandra di for their support and assistance. Gyanranjan, Dheeraj, Animesh, Bijoy, Purbasha di, Mousumi, Arnab, Basita, Dwaipayan, Anushka, Ashoke vai and almost everyone in department of Physics in Jadavpur University was extremely helpful for which I am truly grateful.

Finally, I would like to take the opportunity to acknowledge my family for their constant support through their constant support through thick and thin. I am grateful to Baba (Mr. Nikhil Ranjan Mallick), Ma (Mrs. Kanan Mallick), Didi (Mrs. Ratna Mallick Biswas) and Jamaibabu (Mr. Tapan Kumar Biswas) for their unconditional love and experienced advices which made my life a lot better. I love you all very much and wish to thank you for everything you have done for me.

---------------------------

**Mintu Mallick**

**Date:**

**(Index No: 57/15/Phys./23)**

**Place:**

SRF, Dept. of Physics

Jadavpur University, Kolkata 700032, India

# ***CONTENTS***

# Chapter 1

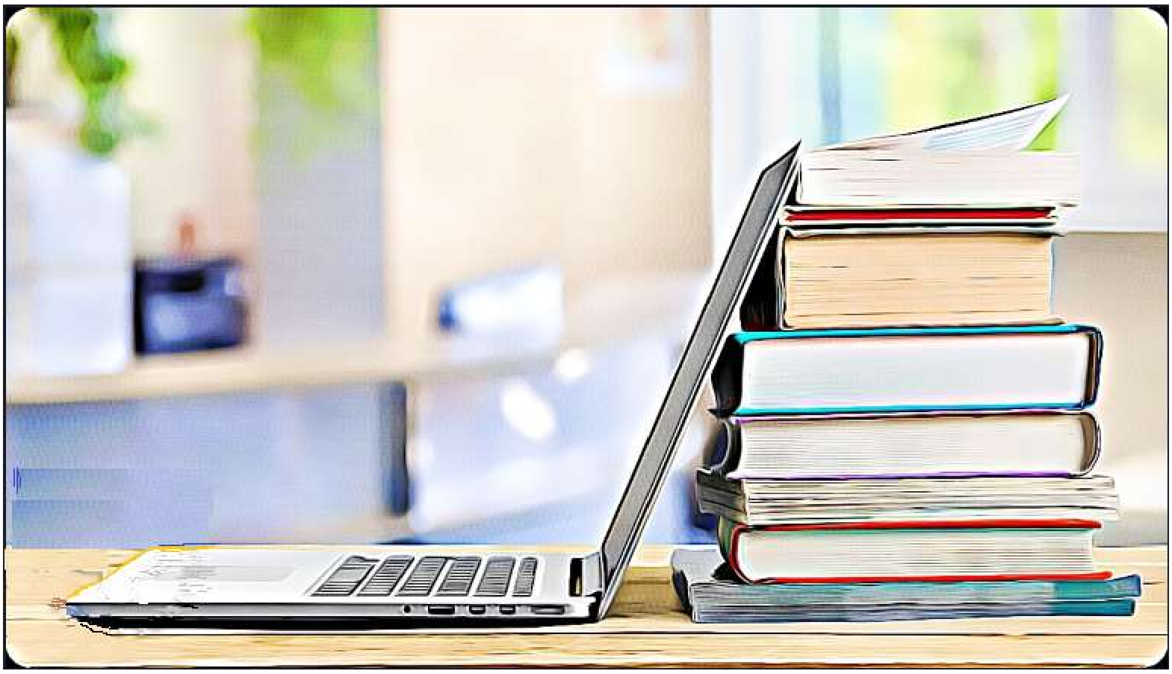

# Chapter 1:
# Review and Scope of Work

## 1.1 Introduction:

Gas sensor (also known as gas detector) is an electronic device that detects the availability of gases in a safety system or an area and has been investigated very interesting sensor devices for many areas of applications including food technology [1]. This sensing technology has been widely used for both indoors or outdoors gas monitoring systems. This kind of equipment is used to find a gas leak in a house, business, or other setting. In 20th centuries some of first investigated a sensor to detect the gases of coal mines (like $CO_2$, CO and $CH_4$) which are causes canary birds down. This yellow colored very songful birds are forgetting to singing and eventually die in presence of this gases [2].

The first inanimate gas sensor was Davy's safety lamp, which is invented by Sir Humphrey Davy in 1815. This safety lamp is used in inflammable atmospheric sphere to reduce the danger of explosions due to the presence of $CH_4$ or other flammable gasses in coal mines [3]. In the year of 1980 to 1990, CO gas detector was discovered by chemically infused paper that turned brown when exposed to the gas. Since then, many devices and technologies have been developed to detect and alert the gas leakage in a wide range of gases [4]. After those various methods had been proposed and applied for gas sensing in industry.

Surface resistance in semiconducting metal oxide gas sensors with thin or thick films that are based on chemical components, surface-modification and microstructures of sensing layers, temperature, and humidity changes in response to the adsorption or desorption of gases. This sensor is known as Conductometric gas sensors [5]. Electrochemical detectors also detect the gas at the same time of gas exposure by measuring the current between two electrodes due to oxidation and reduction process occur [6].

Another important aspect is observation and detection of ethylene gas in fruits, like banana, orange, guava, etc. The smallest plant hormone, ethylene, is essential for numerous plant developmental processes, including fruit ripening, seed germination and flowering, leaf and flower ageing, etc. For the purpose of monitoring the freshness of fruits, a multilayer graphene oxide-based ethylene gas sensor will be created to measure ambient ethylene concentration.

## 1.2 Characteristics of Gas Sensors:

Gas sensors are the crucial components to detect concentration of any types of gas. A set of parameters is used to describe sensor performance. Below is a list of the most crucial criteria along with their definitions.

***Sensitivity:*** It is a measure of how much a response change. This is typically written as the S indicated ratio between the resistance of the gas sensor in the gas and the resistance in normal air. ($S = \frac{Rg}{Ra}$, where Rg represents the resistance of sensing materials at a certain concentration of the target gas and Ra is the resistance of materials in the atmosphere.

***Selectivity:*** When a sensor responds selectively to a set of analytes or even particularly to a single analyte, certain parameters dictate this.

***Stability:*** when the detected gas concentration is constant for a predetermined amount of time, a gas sensor is said to be stable if it can maintain the same output characteristics over that time. This includes retaining the sensitivity, selectivity, response and recovery time.

***Limit of Detection (LOD):*** It is the smallest amount of the analyte that the sensor can detect under the given circumstances, particularly at the specified temperature.

***Repeatability:*** When gas sensors are repeatedly tested in the same testing environment, repeatability refers to how consistently test findings are obtained. Repetition can shorten a sensor's useful life.

***Response Time:*** It is the amount of time needed for a sensor to react to a step change in concentration from zero to a particular concentration value.

***Recovery Time:*** This is the amount of time it takes for the sensor signal to stabilize at its starting point following a step concentration shift from one value to zero.

***Working Temperature:*** Whichever temperature matches its highest sensitivity.

***Life Cycle:*** The life cycle of a sensor is the length of time that it will be used continually.

All of these variables are used to describe a certain material's or device's characteristics. High sensitivity, dynamic range, selectivity, stability, low detection limit, long life, minor hysteresis, and rapid response time are desirable characteristics for a gas sensor.

## 1.3 Classification of Gas Sensing Methods:

Gas sensing technology classifies into two groups [7]: methods based on electrical variation with different material and others, as shown in figure 1.1.

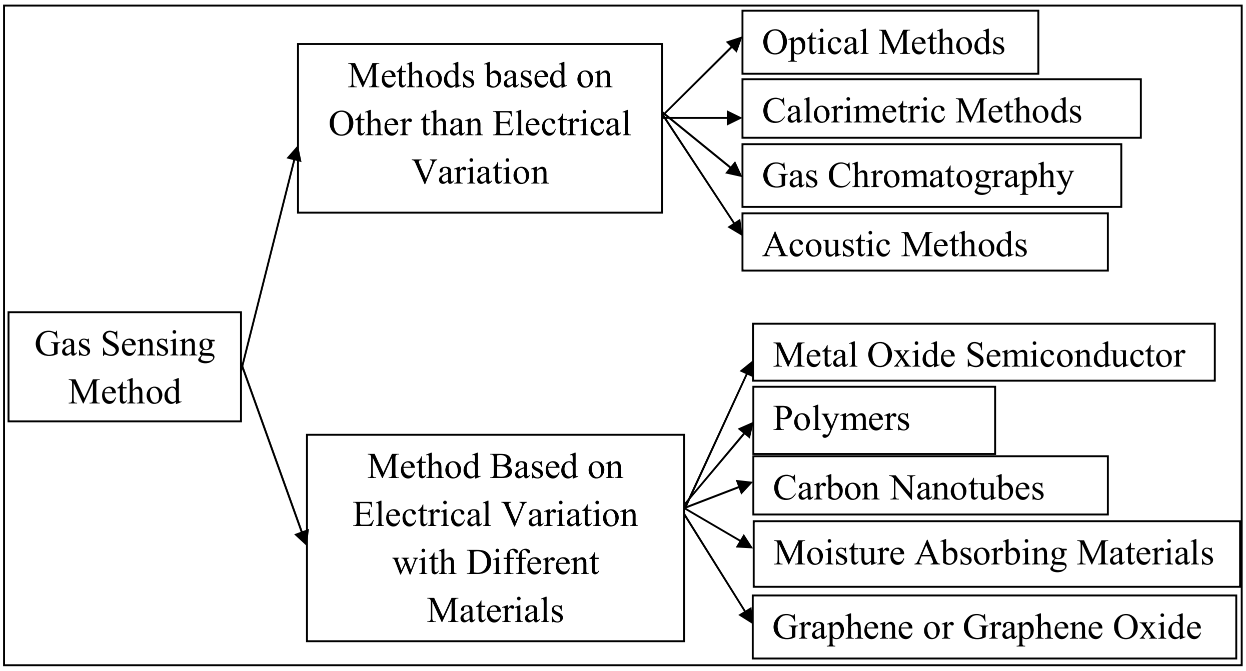

**Figure 1.1:** Classification of gas sensing methods.

### 1.3.1 Methods Based on other Electrical Variation:

#### 1.3.1.1Optical Methods:

Optical method for gas sensing is straightforward with higher sensitivity, selectivity, stability, short response time and longer lifetime than non-optical method. This method's performance won't be affected by environmental changes or other poisons brought on by particular gases. For optical gas sensing, spectroscopy-based techniques are most frequently used. But, the applications on gas sensor of this method are limited due to miniaturization and relatively high cost. So, only very some of commercial gas sensors are based on optical gas sensor principals.

Emission and adsorption of Spectrometry are mainly involves in Spectroscopic analysis. Excited atoms will emit photons and then return to their ground state; emission spectrometry has observed this process. One type of emission spectrometry is called laser-induced breakdown spectroscopy (LIBS). The concentration dependant adsorption of photons at specific gas wavelengths (i.e, Beer-Lambert law) is the principle of adsorption spectrometry. HITRAN database [8] can be found the wavelength for specific gases. Apart from the basic technique according to principles, there are many types of absorption spectrometry including Differential Optical Absorption Spectroscopy (DOAS) [9, 10], Tunable Diode Laser Absorption Spectroscopy (TDLAS) [11], Raman Light Detection and Ranging (LIDAL) [12], Intra-Cavity Absorption Spectrometry (ICAR) [13,14,15], etc. Emission and adsorption both can be used in Furrier Transform Infrared Spectroscopy (FTIR) [16]. Photo-acoustic Spectroscopy and Correlation Spectroscopy are also belonging to spectroscopic analysis.

These techniques are commonly used for gas detector sensors; all are more complicated system design and higher cost to improve excellent sensitivity, selectivity and reliability than other gas detector.

Another optical gas detector technique is Infrared (IR) based basic molecular adsorption spectrometry technique which is widely used. IR source, gas chamber, and IR detector are its three main components. When the source of infrared (IR) emits radiation with a wavelength in particular gas, then gas will absorb the radiation in its particular way. The IR detector detected and measured the presence of interested gas. This system is also known as Non-Dispersive Infrared (NDIR) gas sensor. Apart from the single detector mode, we employ the two-detector layout mode since it is more complex when the ambient environmental elements are removed. Figure: 1.2 depicts the mode of the two detectors.

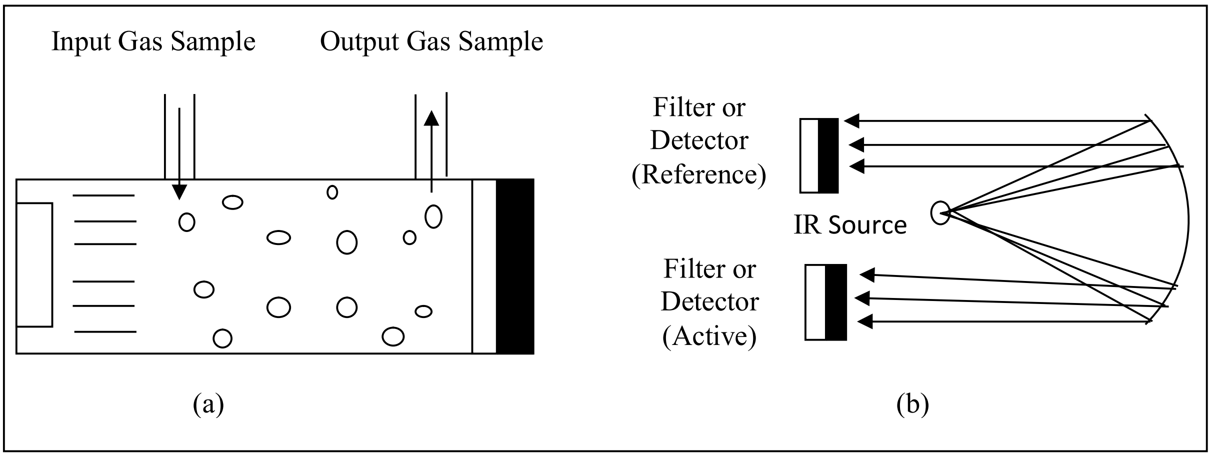

**Figure: 1.2**. (a). Basic IR source gas sensor, (b). IR source gas sensor with reference detector.

[X. Liu, et. Al, A Survey on Gas Sensing Technology, Sensors 2012, pp. 9635-9665]

The IR-source significantly affects the final detection result in each of the three aforementioned methods. Traditional IR sources, however, have serious drawbacks, such as a lack of continuous wavelength tenability, a small output power, complexity, and a lack of nonlinear optical sources with enough power. Numerous laser sources have been studied despite drawbacks, like, Quantum-Cascade Lasers (QCLs) providing excellent tenability, low average power and operated at room temperature. However, long lifetime and insensitive to environment change is the advantages of this methods, but also the disadvantages are followed with it, like high cost and difficulties in miniaturization.

Now, remote air quality monitoring and gas leak detection system is invented with the help of IR-based or NDIR based sensing technology with great accuracy and safety [17, 18]. Due to increasingly extraordinary performance these optical based sensors will dominate the premium market.

### 1.3.1.2 Calorimetric Methods:

Pellistor is a combination of pellet and resistor, it constitutes a major class of electrical gas sensors, which are calorimetric in nature. Here, the detection components are tiny "pellets" of different ceramic catalysts, whose change in resistance in presence of the target gases. The limit of detection for this type sensor is typically in low parts-per-thousand (ppth) range [19], which is not suitable for laboratory applications only applicable for industrial uses.

Basically, two types of pellistors are exists: Catalytic and Thermal Conductivity (TC). The heat evolution from the catalytic oxidation of the gas analyte was monitored by the most popular commercial type of catalytic pellistor sensors. In a short response time, by burning the target gas and generating a specific combustion enthalpy, the detection of low concentration analytes is enabling [20, 21].

On a ceramic bead with a platinum coil acting as a heater or calorimeter, a catalytic layer with a large surface area is applied. With the aid of a platinum coil, the catalytic layer was heated to the point where flammable gas would burn (at around 500 °C). This produced heat can change in resistance of coil and measured by a Wheatstone bridge like simple circuit [22]. The schematic diagram of the catalytic sensor is shown Figure: 1.3.

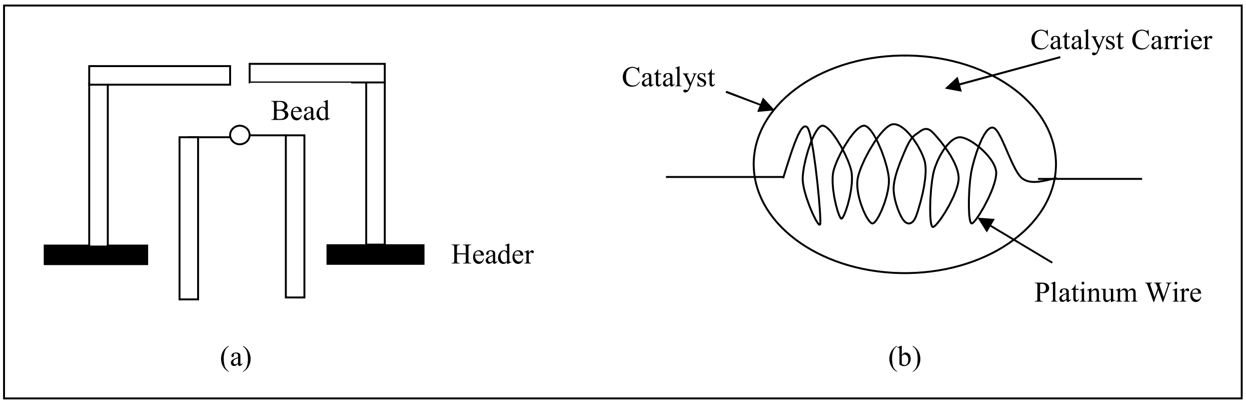

(a) (b)

**Figure: 1.3.** (a) Catalytic Sensor (Schematic diagram) and (b) Configuration of Ceramic Bead.

[X. Liu, et. Al, A Survey on Gas Sensing Technology, Sensors 2012, pp. 9635-9665]

At low temperature with the help of electric field, this sensor could get proper output sensitivity [23], but the process of attenuation of sensitivity in poisoning experiments was slower than that of ordinary catalytic sensors.

The heat dissipation into gas analytes is identified based on their thermal conductivity measurement [24]. The target gas is poured into a gas chamber with a heater in the middle constructed of platinum or tungsten wire. When the chamber's central component is heated with a specific temperature, the component's resistance changes, providing details about the gas and allowing for gas identification. Thermo-conductivity sensors are more effective at detecting things and have a larger detection area. These sensors also have a number of benefits, including strong stability, dependability, and ease of use, although their accuracy and sensitivity still need to be improved.

Enthalpy change methods, which provide chemical reactions that release or absorb heat from the environment, are another calorimetric technique. As various pure gases or mixtures of gases may have identical combustion enthalpies or thermal conductivities, this sensor typically lacks selectivity. The calorimetric sensors, on the other hand, rely on the assumption that the gas constituents are known or present in trace amounts and have sufficiently different physical properties. This allowed for the right selection and calibration of the gas sensors to monitor the analytes.

The following factors need to be taken into account more carefully in order to enhance the functionality of current calorimetric gas sensors for their industrial applications: (a) lowering the power usage and (b) boosting the sensors' ability to withstand mechanical trauma and poisoning.

#### 1.3.1.3 Gas Chromatograph:

Another most common method for gas sensing is Gas Chromatography (CG), but more precisely it is an archetypal laboratory technique having superb separation performance high sensitivity and selectivity [25]. This sensing technique includes subsrantial quantitative analytical methods, such as Volaile Sulphur Compounds (VSCs) could be analyzed by Flame Photometric Detection (FPD), Pulse Flame Photometric Detection (PFPD), Sulphur Chemiluminescent Detection (SCD), and Atomic Emission Detection (AED) [26]. A branch of GC, GC-Olfactometry (GC-O) method [27] fuses human perception of smell and chromatographic separation of compounds. However, GC is relatively expensive, and further technological advancements are required for downsizing for portable applications. Therefore, the device and material restrictions for unattended, flexible fundamental sensors are not entirely satisfied by the GC approach.

### 1.3.1.4 Acoustic Methods:

Gas sensor based on any other principals experience some intrinsic weakness that are difficult to overcome, such as short lifetime, now it could be avoided especially when applied wireless sensor networks by using ultrasonic methods [28]. The three basic areas of this method are acoustic impedance, attenuation, and sound speed.

Time-of-Flight (TOF), which takes into account how long ultrasound takes to travel over a certain distance, is the most reliable detection method for determining the propagation velocity of ultrasonic waves. Figure: 1.4 illustrates an ultrasonic detecting technique. In order to measure the ultrasonic propagation properties, such as the time difference (Δt) or the sound wave phase, two identical channels are filled independently with the reference gas and the gas mixture in the diagram.

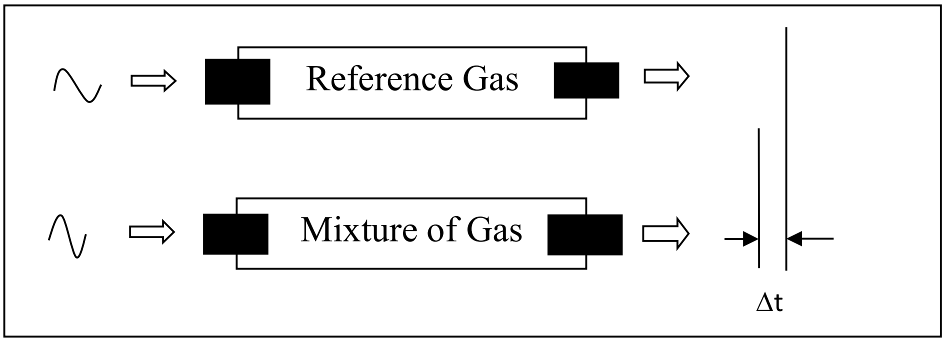

**Figure: 1.4.** Method of ultrasonic detection.

Due to its high-power consumption, traditional ultrasonic gas detection technology has a substantial impact but is particularly challenging to integrate into wireless nodes for ultrasonic gas concentration detection. Researchers have created a better single channel TOF for binary mixes to address this issue. The standard reference speed of sound CR and the resulting time difference (Δt) between transmitting in the air and target gases are calculated using the relationship between the speed of sound in the air and the air temperature [29].

The measured gas velocity can be used to determine many gas properties like concentration of target gas, time difference of propagation of sound [29], and identify a gas through which the sound velocity is different from other in a mixture of gases [30], and calculate the molar weight of different gases in a mixture based on some equations of thermodynamics [31, 32, 33].

When an acoustic wave travels through a medium, the energy loss (like thermal and scattered energy) is called attenuation [34]. Because different gases exhibit varied attenuation qualities and because different gas properties can be determined, this aids in the detection of individual gases. But compared to the sound speed method, which is affected by noise, gas-borne particles, and even transducer deterioration with time, attenuation is a significantly less reliable technique. Due to these factors, acoustic attenuation is just a small portion of commercial gas sensors.

Acoustic impedance is a different sensor technique that is typically used to calculate gas density. Its equation is $Z=\rho C$, where $\rho$ is gas density and $C$ is sound speed. Here, using observed acoustic impedance and the speed of light, the density of a gas could be estimated [35]. Therefore, it is highly challenging to quantify a gas's acoustic impedance in a natural setting. As a result, commercial acoustic sensors have not typically used attenuation and acoustic impedance.

## 1.3.2 Methods Based on Electrical Properties:

### 1.3.2.1 Metal Oxide Semiconductor:

Metal Oxide Semiconductor (MOS) is one of the sensing materials which have various advantages like low cost, high sensitivity and others. This gas sensors are the most investigated groups of gas sensors. These are the most typical sensing materials, and they offer sensors various benefits like high sensitivity and inexpensive cost. It falls into two groups: Transition versus Non-Transition. As much more energy is needed to form other oxidation states, the non-transition (e.g., $Al_2O_3$) contains elements with only one oxidation state while the transition (e.g., $Fe_2O_3$) contains more oxidation states [36]. The transition metal oxides, which are used as sensing materials by metal oxide semiconductors, are visible when the two metal oxides are compared because they can produce various oxidation states on the surface. The transition-metal oxides with $d_0$ (transition metal oxide, like; $TiO_2$, $V_2O_5$, $WO_3$) and $d_{10}$ (post-transion-metal oxide, like; $SnO_2$ and ZnO) electronic configurations can be used in applications of gas sensing [37]. The most prevalent metal oxide semiconductors that are sensitive to gas concentration are N-types. There are a few kinds of p-types semiconductors also like $NiO_x$ (usually doped with n-type semiconductor like; $TiO_2$) which could be used as gas sensor sensing materials. 10% weight NiOx content is necessary to change n-type conductivity into p-type conductivity. As temperature increases the sensitivity of n-type towards reducing gases is increased while that of the p-type is decreased, this is the main difference between n-type and p-type $NiO_x$ doped $TiO_2$ film [38]. So, n-type semiconductors have relatively higher operating temperatures than p-type ones. To detect target gases through redox reactions between the target gases and the oxide surface, sensors which are based on metal oxide semiconductors are mainly applied [39]. The two phases that make up this process are (a) redox reactions, in which molecules of the target gases react with O-distributed on the surface of the materials, and (b) transduction into an electrical resistance variation of the sensors. Calculating changes in capacitance, work function, mass, etc. could be used to identify changes in resistance [37].

$TiO_2$, $SnO_2$, CuO, $V_2O_5$, all are the metal oxide could be utilized to detect combustible, reducing or oxidizing gases which are mainly based on the change in resistance response to the target gases [40]. Titanium dioxide ($TiO_2$) is commonly used as a gas sensing material which have sensitive layers for their sensitivity in terms of dielectric permittivity to gas adsorption [41]. Tin oxide ($SnO_2$) is a different form of sensing material whose conductivity depends on the density of oxygen ions that have been pre-adsorbed on the surface. According to variation gas concentration the change of resistance of tin oxide changes, while the relationship between resistance changes and gas concentration is measured [42]. Other metal oxide semiconductor is tungsten trioxide ($WO_3$) applying electrochemical etching of tungsten shows excellent responses towards hydrogen and nitrogen oxide [43].

Due to its great availability and high sensitivity, $SnO_2$ based gas sensors have a very high sensitivity compared to all other types of gas sensors based on metal oxide semiconductor. Therefore, its high working temperature, which was realized as a headed filament, is the primary cause of the great sensitivity. The working temperature of $SnO_2$ based sensors is from 25° to 500 °C.

Gas sensors made of metal oxide semiconductors are frequently employed. In comparison to sensors that operate at ambient temperature, some sensors that require high operating temperatures require more expensive and complex designs. Micro-sized sensor elements with micro-heaters have been developed by researchers and are being tested with IC technology. Another issue is the prolonged recovery period required after gas exposure, as well as the numerous limitations on their use in situations where gas concentrations may fluctuate quickly. Their range of use is also constrained by other indicators' structural instability and flaws.

### 1.3.2.2 Polymers:

Polymer-based on sensors are mainly applied in detecting inorganic gases like $CO_2$ and $H_2O$ [44] and also used to detect a wide range of volatile organic compounds (VOCs) or solvent vapour in gas phase, like alcohols, aromatic and halogenated compounds. The physical characteristics of polymer layers, such as their mass and dielectric properties, will alter following gas adsorption when they are exposed to an analyte's vapour. According to significant variations in physical properties, polymers utilised for gas sensing can be further separated into two groups: conducting polymers and non-conducting polymers.

***Conducting Polymers*****:** Conducting polymers are the focus of much research due to their extraordinary qualities, such as tunable electrical properties, high optical and mechanical capabilities, simplicity of synthesis and fabrication, and superior environmental stability to conventional inorganic materials. It is well known that exposure to various organic and inorganic gases can influence the electrical conductivity of these conducting polymers [45]. This feature has led to the investigation of these materials as gas sensing layers by a number of groups [46,47,48]. It could be used as a gas sensing material such as polypyrrole (PPy), polyaniline (PAni), polythiophene (PTh) and their derivatives [49]. More work needs to be done in order to realise the function of sensing gases.

***Non-Conducting Polymers*****:** Thanks to polymers, numerous sensing devices are frequently used as sorptive coatings. In this instance, the device can be compared to a typical transducer. Polymer films that change with analyte absorption or desorption in terms of resonance frequency, dielectric constant, and enthalpy may be used to cover mass-sensitive sensors. The sensor device could then emit an electrical signal as a result of changes in the observed polymer characteristics [50]. Even when coated on sensor devices with the same qualities, the performance of non-conducting polymers in gas sensing is more challenging than their basic principles would suggest. By introducing the sensitivity of polymer layers, non-conducting polymer membrane, such as polyimide, might be employed on metal oxide semiconductor gas sensors as molecular sieves to increase overall selectivity. High sensitivity and short response times are the advantages of polymer-based gas sensors but operated only is in room temperature. Additional benefits of polymers include low fabrication costs, simplicity, and reproducibility.

Other limitations of polymer-based on gas sensors include long-term instability, irreversibility, poor selectivity, and the potential for working circumstances to affect performance. However, a more thorough and comprehensive justification of the operating principles of polymer as sensing materials is still required. However, polymer-based sensors for gas sensors will have a promising future due to their lower power consumption.

### 1.3.2.3 Carbon Nanotubes:

Due to their high surface area, size, and hollow geometry, carbon nanotubes (CNTs) have been effectively used as prospective options for constructing gas and chemical sensors [51]. At room temperature, CNTs have gained increased attention because of their distinctive properties and have emerged as the most promising materials for extremely sensitive gas sensors, while conventional sensing materials like metal oxide semiconductors must cope with the issue of inadequate sensitivity. While other materials, like metal oxides, require additional heating to function normally, CNTs have been discovered to have electrical properties and to be highly sensitive to extremely small quantities of gases, such as alcohol, ammonia ($NH_3$), carbon dioxide ($CO_2$), and nitrogen oxide ($NO_x$) at room temperature [52].

Similar to other gas sensing components, CNTs have various response times and properties depending on the target gas. In both physisorption and chemisorption, the response property varies. In the case of $CO_2$ and $O_2$, it has been shown that the reaction is linear and reversible, proving that the only process at work is physisorption. But the response to $NH_3$ is both irreversible and reversible, demonstrating that the CNTs can adsorb $NH_3$ both physically and chemically. Additionally, the response periods to various gases vary [53].

In order to enhance the sensitivity and selectivity, CNTs are often coupled with other materials. CNTs could be mixed with silane to improve the sensitivity and mechanical adhesion to the substrate [54]. For sensitivity enhancement, olgonucleotides (DNA, RNA) may be utilized. The length of DNA sequence impacts the response process of CNT gas sensors [55]. Incorporation of CNTs into other sensing materials such as metal oxide semiconductors improve sensitivity [56]. Incorporation of CNTs.

The use of CNTs is being expanded to include the detection of partial discharges (PD) caused by the breakdown of Sulphur hexafluoride ($SF_6$). PD is a useful technique for evaluating the insulation state of gas-insulated switch gear (GIS). Another graphene-based gas sensor has also found to be a good gas adsorbate. The crystal defects maximize the signal to noise ratio to a level sufficient for detecting variations of gas concentrations at room temperature [57].

CNTs and graphene are two examples of novel materials that have promise for the future. Additionally, there are several drawbacks to these gas sensors, including high manufacturing costs and challenges with repeatability and fabrication.

#### 1.3.2.4 Moisture Absorbing Material:

Moisture-absorbing materials could be implanted with RFID tags in order to detect water vapor concentrations, which is the level of humidity, because their dielectric constant can be changed by the presence of water in the environment. Typically, the RFID tag antenna is coated with materials that resemble paper. The near-field ohomic losses caused by the water absorption change the resonance frequency of the tag antenna, which is detected by RFID readers. The minimal power level provided by the RFID reader to power up the tags for passive RFID tags depends on the water content, which can be described in terms of the humidity of the surrounding air. This method might just require one tag, but the spacing between tags and readers must be constant. An alternative technique involves using two tags at once, one of which is protected from moisture-absorbing substance and the other which isn't. A table showing how the power-up level differs from the water concentration is required for this procedure [58].

These sensors could be placed inside the floors or walls of buildings to stop costly mould or decay-related damage. These sensors could find leaks if placed underneath covert water pipes [59].

Moisture-absorbing materials may be used as the antenna's substrate rather of just the tag's cover since the dielectric constant of an RFID tag antenna can be influenced by the air's humidity level. This would result in performance variations that an RFID reader could detect. Tags wrapped in moisture-absorbing material are inexpensive and ideal for mass manufacture. In high humidity, the drawbacks of moisture-absorbing material-based gas sensors are susceptible to friction and may become irreversible.

### 1.3.2.5 Graphene and Graphene Oxide:

Due to their enormous specific surface areas, high conductivity, and atom-thick two-dimensional conjugated conjugated architectures, graphene materials have been extensively investigated for the production of gas sensors [60, 61]. The methods used to create graphene materials for this purpose and the most recent developments in their production are summarized in this feature article [62].

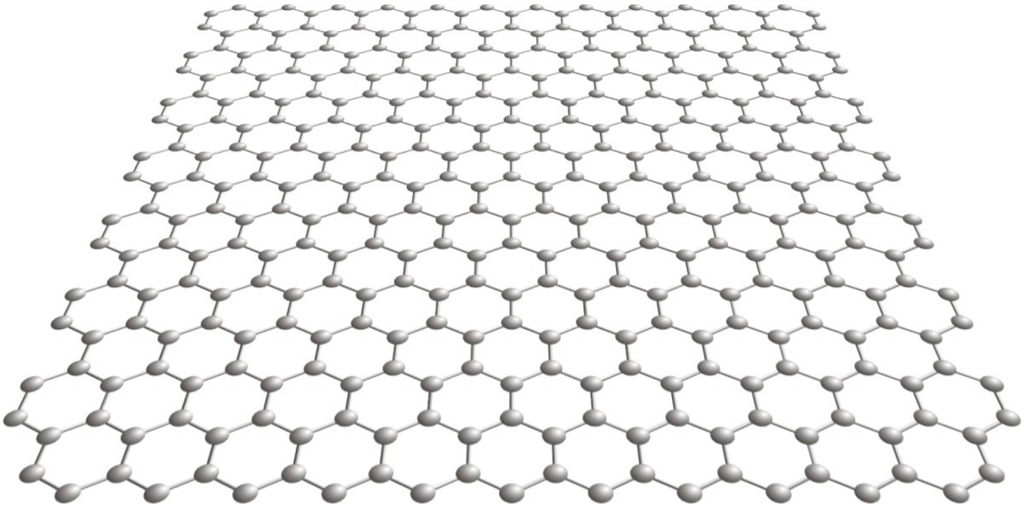

**Figure: 1.5** Two-dimensional Graphene.

Other applications for graphene-based nanoelectronic devices include strain and pressure sensors, PH sensors, environmental contamination sensors, DNA sensors (for detecting nucleobases and nucleotides), gas sensors (for detecting different gases), and others.

**Graphene Oxide (GO)** also called Graphitic Oxide is a single-atomic layered 2D honey-comb lattice material, made by the powerful oxidation of graphite with the help of $KMnO_4$ and $H_2SO_4$, which is cheap, abundant and easier to manufacture than Graphene [63, 64, 65]. It is an oxidized version of graphene having functional groups that contain oxygen (like oxygen, hydroxide, etc). It is soluble in water and other solvents and can be used to make graphene. There are techniques to make graphene oxide a better conductor despite its poor performance. Due to its enormous surface area, it can be used as an electrode material for batteries, capacitors, solar cells, and other gas sensors. It is frequently used as a coating on substrates, in powder form, or dispersed.

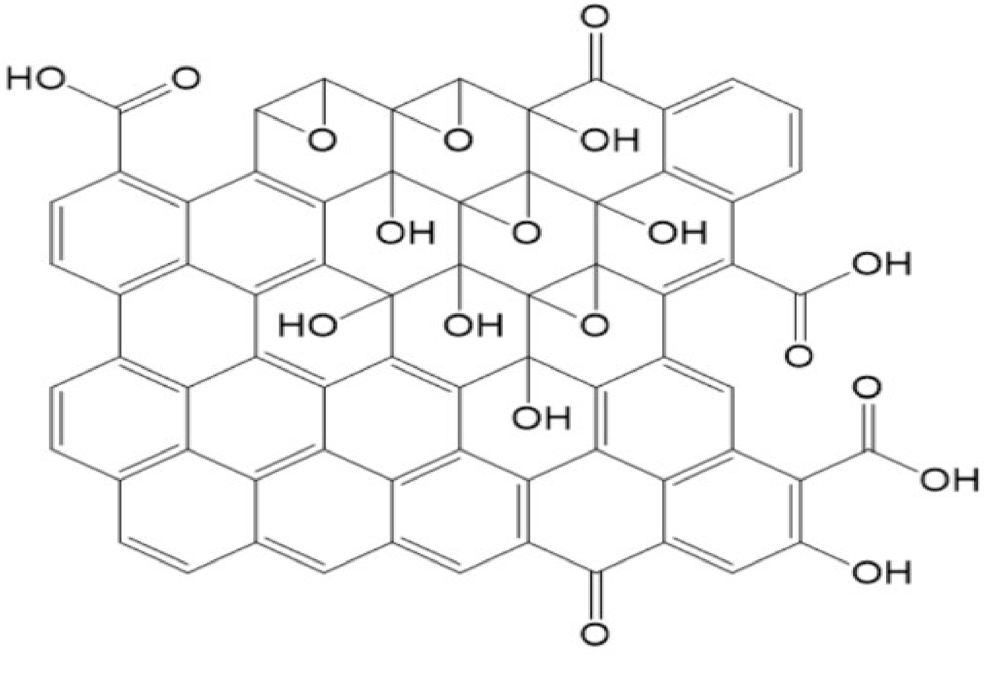

**Figure: 1.6** Two-dimensional Graphene Oxide.

## 1.4 Synthesis of Graphene Oxide:

There are four fundamental ways to make graphene oxide: (a) Staudenmaier, (b) Hofmann, (c) Brodie, and (d) Hummers. There are numerous varieties of these techniques, and new developments are continuously being investigated to produce better outcomes and more affordable procedures. The carbon/oxygen ratios of the graphene oxide are frequently used to assess the efficacy of an oxidation process.

### 1.4.1 Staudenmaier and Tour Method:

First, 1 gm of natural flake graphite was mixed with 27 ml of 2:1 percentage of $H_2SO_4$ and $HNO_3$ mixture in an ice-cooled glass jar. The maintained temperature was below the 35 °C with slowly adding 11gm of $KClO_3$. After 96 hours, added 800 ml of water to the solution with continuous stirring and filtered using 0.45 µm of nylon membrane. To remove the sulfate ions, the prepared mixture was repeatedly washed with 5% HCl solution. And to pull out chloride ions, the mixture was washed repeatedly with DI water. Finally, Graphene Oxide was prepared with the help of Staudenmaier method [66, 67].

Tour method, where 1gm of natural flake graphite mixed with percentage of 9:1 of $H_2SO_4$ and $H_3PO_4$ with continuous stirring for 3 minutes. Then, added 5gm of $KMnO_4$ and the reaction temperature was maintained at 20 °C for 3 days. Decanted of sulfuric acid the mixture was centrifuged at 5000 rpm for 30 minutes. Finally, washed with water in some times and centrifuge at 5000 rpm, then Graphene Oxide is prepared [68, 69].

### 1.4.2 Hofmann Method:

A Pyrex beaker (reaction flask with thermometer) was used to combine 87.5 ml of sulfuric acid (98%) and 27 ml of nitric acid (68%) before the mixture was chilled in an ice bath for 30 minutes. After then, 5gm of graphite powder was continuously stirred into the mixture. In order to prevent a quick rise in temperature and the creation of explosive chlorine dioxide gas, 55gm of potassium chlorate was then gradually added to the mixture. The mixture was continually stirred for 96 hours at room temperature after the potassium chlorate had dissolved. After the reaction was finished, the mixture was added to 3 lit of DI water. We repeatedly centrifuged with DI water while adding 5% HCl to remove sulphate ions until a negative reaction between chloride and sulphate ions was achieved. Before usage, prepared graphene oxide was then dried for 48 hours in a vacuum oven at 60 °C [67, 70, 71].

### 1.4.3 Hummer's method:

Before usage, a Teflon reactor, $KMnO_4$, sulphuric acid (98%) and graphite powder were thoroughly cooled in a refrigerator at 0–4 °C. An autoclave made of stainless steel contained the Teflon reactor. Sulphuric acid (600 ml) was then added to the reactor along with the cooled graphite (20 g) and $KMnO_4$ (80 g). The stainless-steel autoclave and reactor were covered as soon as the sulphuric acid was poured. The autoclave was held at 0–4 °C for 1.5 hours before being heated in an oven for 1.5 hours at 100 °C. With 10 L of water, the obtained mud was thinned. $H_2O_2$ (30%) was slowly dripped into the suspension while being stirred mechanically until the slurry turned golden. The suspension was washed with hot HCl and deionized water until the pH reached 7, and humid GO was obtained [72, 73, 74].

### 1.4.4 Modified Hummer's Method:

The well-known Hummer's approach [74–77] is another straightforward technique for producing graphene oxide (GO). In this procedure, 50 ml of $H_2SO_4$

(98%) was combined with 2 gm of pure graphite powder and 2 gm of sodium nitrate while being continuously stirred in a borosil beaker. 6 grammes of $KMnO_4$ were added very gradually after an hour, with the rate of addition being carefully managed to keep the reaction temperature below 15 °C. After that, the ice bath was withdrawn, the temperature was allowed to rise to 35 °C, and it was stirred continuously for two hours to create a brownish paste. Then, 100 ml of pure distilled water was progressively added, causing the temperature to rise quickly to 95 °C and the liquid to turn brown. Additionally, this solution was made diluted by continuously swirling in an additional 200 cc of water. We added 10 ml of $H_2O_2$ to stop the reaction, and the color turned yellow. The solution was rinsed with 10% HCl and de-ionized (DI) water at room temperature until the pH of the solution reached 6. Finally, the precipitate was collected after filtration and dried at room temperature.

## 1.5 Graphene Oxide as a Gas Sensing Material:

One type of nanomechanical sensor used grapheme oxide (GO) as a gas detecting material and operated in static mode as a sensing platform. Chemically altered graphene with low conductivity can be employed as a gas detecting material since membrane type surface stress sensors pick up surface stress brought on by gas sorption. The gas-sensing materials graphene and reduced graphene oxide (RGO) are well known, but the appealing sensing material known as graphene oxide (GO) has also been extensively researched in recent years. When exposed to particular gases, GO materials' electrical or optical properties change, and the functional groups on GO nanosheets are essential for adsorbing gas molecules. GO materials can be enhanced in terms of sensitivity and selectivity to analyte gases using metal nanoparticles and metal oxide nanocomposites. Applications of GO-based sensors include the detection of organic vapors, water vapor, $NO_2$, $H_2$, $NH_3$, and $H_2S$.

***Humidity sensor using by GO:*** A typical application of GO is humidity detection. GO is very hydrophilic and proton conductive, which makes it a superior material for water vapor sensing like the conventional proton conducting material, in contrast to graphene and RGO [78, 79, 80]. Guo et al. produced GO sheets for humidity sensing on a flexible polyethylene terephthalate film in 2012 [81]. They used a model sheet with 32 carbon atoms to calculate the binding energies of water on graphene materials. Graphene with water have a modest Van-der-Waals interaction (0.044 eV), although water forms hydrogen bonds with epoxy (0.201 eV) and hydroxyl groups (0.259 eV). The electrical conductivity and response/recovery time were controlled while patterning the material mask-free using a two-beam laser interference treatment. The formation was managed to achieve this.

***$NO_2$ gas sensing by GO:*** Ozone treated graphene (OTG), which was created by Chung et al. [83] for $NO_2$ sensing, is the first use of GO as a gas sensor. While GO is typically synthesized using the Hummers method, this sensor was created by depositing a thin layer of graphene using chemical vapor deposition (CVD) [84] and then oxidizing it with $O_3$ treatment [85]. The oxygen groups' higher $NO_2$ binding energy improved molecular affinity and boosted reaction intensity, but recovery degraded as a result. Low for sp2-bonding carbon (0.05-0.4 eV) and high for oxygen groups (0.4-8 eV) are the binding energies of $NO_2$ molecules [86, 87]. As a result, OTG has better affinity for $NO_2$ than regular graphene; for 200 ppmv of $NO_2$, OTG's percentage resistance change was nearly twice as great as that of pristine graphene. Higher temperatures were preferable for recovery time, whereas lower temperatures were preferable for percentile resistance change. The Langmuir adsorption isotherm theory was used by the authors to explain the $NO_2$ adsorption/desorption mechanism, including temperature effects. The reported estimated limit of detection (LOD) for the OTG sensor was 0.0013 ppmv, and it responded to $NO_2$ concentrations between 0.2 and 200 ppmv.

Prezioso et al. [88] reported the development of another $NO_2$ sensor that was made by casting a GO solution made from graphite flakes with a maximum size of 500 µm using a modified Hummers process [89]. The authors demonstrated how temperature affected the GO resistance behavior. As the working temperature rose in dry air, the resistance dynamically reduced. Stable baselines were established between 25 and 150 °C, and higher temperatures produced stronger reactions and recoveries. At room temperature, however, both reactions and recoveries were unacceptably slow. However, the oxygen functional groups vanished as the operating temperature surpassed 200 °C, which reduced the sensing capacity. The scientists came to the conclusion that annealed GO was inferior to as-deposited GO and that 150 °C was the ideal temperature for sensor performance. Due to the fact that $NO_2$ molecules preferentially adsorb on them, the oxygen functional groups play a significant role in the gas sensing active sites. The oxygen functional group's negative charge transfers to the $NO_2$ molecule, giving rise to a positively charged vacancy in the honeycomb structure below. Exposure to $NO_2$ thereby increased the conductivity of the GO. The strength of the NO2 signal was inversely related to the logarithm of the $NO_2$ concentration and ranged from 10 ppmv to 0.02 ppmv..

Prior to looking into GO sensors, graphene and RGO-based sensors for $NO_2$ detection were researched [90]. By placing a transient voltage across RGO to create pits and epoxide and ether functional groups like GO, Cui et al. increased the sensitivity of sensors to $NO_2$ [91]. Li et al. [92] also looked at NO detection using RGO. Responses for NO as low as 0.002 ppmv were shown, demonstrating the high sensitivity of palladium decollated RGO to NO. They put out a conductivity change model in which adsorbed NO lowered the Schottky barrier that formed between Pd and RGO.

Other articles [93, 94] reported on the performance for $NO_2$ and $NH_3$ detection, and used $Co_3O_4$-intercalated RGO [95] to detect $NO_2$ and $CH_3OH$. RGO, in contrast to GO, was sensitised with additions such sulfonate, ethylene diamine, Ag-nanoparticles, $Cu_2O$ nanowire meso crystal, $SnO_2$, ZnO nanoparticles, Pd, $Co_3O_4$, and others. The RGO sensors' resistivity reacted unfavorably to $NO_2$ and favorably to $NH_3$ and methanol.

***$H_2$ sensing by GO material*:** Hydrogen is a dangerous yet necessary gas that is used in gas chromatography, chemical reduction, and as a carrier gas in industrial processes. When exposed to $H_2$ gas, RGO itself functions as an $H_2$ sensing material and changes in optical characteristics [96]. RGO combined with Pd, Pt, Pd-$WO_3$, and ZnO nanocomposite materials [97, 98]. The responses of Pd (3 nm), which was sputtered over RGO (2 nm) made from GO, were proportional to the logarithm of the $H_2$ concentration between 200 and 3300 ppmv [99]. According to the most recent study by Du et al., the Schottky junction between silicon and Pd-RGO changed when exposed to $H_2$, which led to a decrease in device resistance when $H_2$ was present [100]. In addition to the RGO-based $H_2$ sensors that were previously addressed, GO-based $H_2$ sensors have also been produced. Pustelny et al. from Poland looked into the $H_2$ and $NO_2$ sensitivity of GO [101]. Inter digitated Au/Cr electrodes were created using the lift-off method and electron beam physical vapor deposition (EBPVD) to test the GO sensing capabilities. This sensor responded to $H_2$, but the temperature had a significant impact on the behavior. On the other hand, with $H_2$ concentrations between 1% and

4% at 120 °C, good reactions were obtained. Both $NO_2$ and $H_2$ were detected by this sensor, and both gases caused negative resistance changes; however, $NO_2$ was more easily detected at lower temperatures. Although a suitable sensor for measuring $H_2$, humidity correction is advised.

To create a more sensitive $H_2$ sensor, Wang et al. used dielectrophoresis (DEP) to construct a GO nanostructure [102]. To make GO flakes smaller, a GO suspension was ultrasonically treated for 24 hours right before the DEP procedure. However, the improved sensor performed exceptionally well at $H_2$ concentrations of 100–1000 ppm; percentile resistance changes were, respectively, 4.5, 5.5, and 6.5% at 100, 500, and 1000 ppm. Response and recovery times were correspondingly 55–70 and 80–120 s.

***$H_2S$ and acetone sensing of GO:*** Recently, GO-based sensors for use in healthcare have been studied. Using $SnO_2$ nanofibers functionalized with RGO [103] and hemi tube-structured $WO_3$ that was hybridized with thin graphite (TG) or GO, Choi et al. investigated the detection of $H_2S$ in breath. For sensor preparation GO suspensions mixes with nanostructured metal oxide materials, such as hemitube-structured $WO_3$ and $SnO_2$ nanofiber were respectively used. Although the improvement offered by GO was less than that of TG, the resistance was steady compared to the TG-modified sensor's, whose resistance varied significantly with temperature. TG and GO both serve as electronic sensitizers for the $WO_3$ gas sensing layer. With a response time of less than 15 seconds and a recovery time of less than 30 seconds, the hybridized sensors react quite swiftly. As a result, GO works well as a sensitizer for metal oxide gas sensors.

## 1.6 Ethylene Sensor:

It is well recognized that ethylene treatment is an efficient approach for treating fruits after harvest. a gas sensor using a silicon carbide-based field effect transistor (SiC-FET) for measuring the concentration of ethylene gas produced by fruits. By adjusting the operating temperature, gate material, and material structure, SiC-FET sensors' selectivity and sensitivity can be adjusted toward a small number of target gases. The iridium gated SiC-FET sensor is highly sensitive to ethylene, and the greatest response is attained at a temperature of 200 °C [104].

A flexible semiconductor with potential use in the field of sensing is zinc oxide (ZnO). Detecting ethylene is important in agriculture to minimize losses during the storage of fruits and vegetables. In this study, chemical co-precipitation was used to make ZnO nanocrystals, which were then used as ethylene sensors. A large response of 11.7 was shown by a ZnO nanocrystal-based sensor at ambient temperature and about 70% relative humidity. For ethylene gas, the ZnO nanocrystal-based sensor's detection threshold was 10 ppm. The adsorption performance was simulated via the first principles study based on the density functional theory to explain the sensing mechanism [105].

The porous ZnO nanosheets display a reasonable level of sensing capabilities as well as a dramatic response in ethylene detection, combining the advantages of their ultrathin and single-crystalline structure. For ethylene sensors, the quickest response and recovery times are 8 and 20 seconds, respectively. It is anticipated that the porous ZnO nanosheets would open up new possibilities for the creation of cutting-edge nanomaterials for actual use in ethylene monitoring during fruit ripening [106]. In the past few years, a number of studies on ethylene-based fruit maturity monitoring have been published. Current methods for the detection and monitoring of ethylene gas levels include gas chromatography, electrochemical sensing, and laser-based photo-acoustic spectroscopy. All of these ethylene gas sensors are expensive and difficult to use for on-filed applications.

## *1.7 Scope of work of the present work:*

In our daily life, fruits are very essential, but perfect ripe fruits are not so easy to identify by observing the change of colour in natural way, it turns into brown or blackish and futile very fast. In United States only, about 20% of all produced fruits and vegetables are lost due to spoilage in every year [107].

Unsaturated non-polar hydrocarbon, ethylene ($C_2H_4$) is a small plant hormone, regulates many developments process of plants [108]. This gas is quite helpful to quickly ripen fruits and vegetables [109]. The internal concentration of ethylene from fruits can indicate the proper time of harvest [110, 111] and detecting atmospheric ethylene level in a storage chamber we can avoid over ripening of fruits before transportation.

Ethylene gas concentration is now monitored via gas chromatography detection, electrochemical sensing [112] or laser acoustic spectroscopy [113], all of these are very expensive and are not suitable for in-field measurement.

To track the freshness of fruits, we have created a multilayer graphene oxide-based conductive type ethylene gas sensor in this study. And clearly identified distinct fruits with the same mass in ideal ripening conditions, thus they can be employed in e-nose applications to distinguish between different ripe fruits. Our graphene oxide pallet sensor shows sensitivity and reliable ethylene gas sensing performance. The sensor shows capability of lower resolution from standard resolution from standard MSR sensor with good reproducibility. Further work will be integrated with commercially available Radio Frequency Identification Device (RFID) tags, which enables it to monitor wirelessly the condition of fruits.

## Reference:

1. B. Kuswandi, Y. Wicasono, Jayus, A. Abdullah, L. Yook, H. M. Ahmad, Smart packaging: sensors for monitoring of food quality and safety, Sensing and Instrumentation for food quality and Safety, ISSN 1932-7587, Volume 5, 2011, pp. 137-146.

2. C. Pollock, DVM, The Canary in coal mine, Journal of Avian Medical and Surgery, 2016, pp. 386-391. https://doi.org/10.1647/1082-391.

3. J. M. Thomas, Sir Humphry Davy and the coal miners of the world: a commentary on Davy (1816) 'An account of an invention for giving light in explosive mixtures of fire-dampe in coal mines', The Royal Society Publishing, Royal Socciety A 373: 20140288, http://dx.doi.org/10.1098/rsta.2014.0288.

4. K. Rekha, R. Kiruthiga, Gas Leakage Alerting and Accident Control System Using GSM/GPS Technology, International Journal of Science and Research (IJSR), ISSN: 2319-7064, 2015, pp. 997-1001.

5. C. Wang, L. Yin, L. Zhang, D. Xiang, R. Gao, Metal Oxide Gas Sensors: Sensitivity and Influencing Factors, Sensors 2010, 10, pp. 2088-2106.

6. A. Thakur, G. Kalaimagal, Intelligent Monitoring System for Carbon Monoxide Poisoning and Leakage in Mines, ISSN: 2248-9622, Vol. 4, Issue 3 (Version 1), March 2014, pp.791-797.

7. X. Liu, S. Cheng, H. Liu, S. Hu, D. Zhang, H. Ning, A Survey on Gas Sensing Technology, Sensors 2012, 12, pp. 9635-9665.

8. I. E. Gordon, L. S. Rothman, R. J. Hargreaves, R. Hashemi, E. V. Karlovets, F. M. Skinner, E. K. Conway, C. Hill, R. V. Kochanov, Y. Tan, P. Wcisło A. A. Finenko, K. Nelson, P. F. Bernath, M. Birk, V. Boudon, A. Campargu, The HITRAN2020 molecular spectroscopic database, Journal of Quantitative Spectroscopy & Radiative Transfer, 2022, pp. 1-82.

9. H. Zheng, Experiment study of continuous emission monitoring system based on differential optical absorption spectroscopy. In Proceedings of 2008 International Workshop on Education Technology and Training and Geoscience and Remote Sensing (ETT and GRS), Shanghai, China, 21–22 December 2008, pp. 175–177.

10. Y. Wang, K. Wang, Q. Wang, F. Tang, Measurement of CH4 by differential infrared optical absorption spectroscopy, Proceedings of the 9th I.C.E.M.I, Beijing, China, August 2009, pp. 1761–1766.

11.Y. Miao, Q. Yao, N. Qiu, J. Zhang, Application research of laser gas detection technology in the analysis of Sulphur hexafluoride. (CICED), Nanjing, China, September 2010, pp. 1–3.

12.T. J. Koplin, M. Siemons, C. Océn-Valéntin, D. Sanders, U. Simon, Workflow for high throughput screening of gas sensing materials, Sensors 2006, 6, pp. 298–307.

13. K. Liu, T. Liu, J. Jiang, G. Peng, H. Zhang, D. Jia, Y. Wang, W. Jing, Y. Zhang, Investigation of wavelength modulation and wavelength sweep techniques in intracavity fiber laser for gas detection. J. Light. Technol. 2011, 29, 15–21.

14. H. Y. Ryu, W. K. Lee, H. S. Moon, H. S. Suh, Tunable erbium-doped fiber ring laser for applications for infrared absorption spectroscopy. Opt. Commun. 2007, 275, 379–384.

15. K. Liu, W. Jing, G. Peng, J. Zhang, Y. Wang, T. Liu, D. Jia, H. Zhang, Y. Zhang, Wavelength sweep of intracaivity fiber laser for low concentration gas detection, IEEE Photon. Technol. Lett, 2008, 20, 1515–1517.

16. V. Arunajatesan, B. Subramaniam, K. W. Hutchenson, In situ FTIR investigations of reverse water gas shift reaction activity at supercritical conditions. Chem. Eng. Sci. 2007, 62, 5062–5069.

17. W. Baetz, A. Kroll, G. Bonow, Mobile Robots with active IR-optical sensing for remote gas detection and source localization. IEEE International Conference on Robotics and Automation (ICRA), Kobe, Japan, May 2009; pp. 2773–2778.

18. J. Kwon, G. Ahn, G. Kim, J. C. Kim, H. A. Kim, study on NDIR-based CO2 sensor to apply remote air quality monitoring system, *ICCAS-SICE*, Fukuoka, Japan, 2009, pp. 1683–1687.

19. X. Liu, S. Cheng, H. Liu, S. Hu, D. Zhang, H. Ning, A Survey on Gas Sensing Technology, Sensors 2012, 12, pp. 9635-9665; doi:10.3390/s120709635.

20. S. Kulinyi, D. Brandszájsz, H. Amine, M. Ádám, P. Fürjes, I. Bársony, C. Dücso, Olfactory detection of methane, propane, butane and hexane using conventional transmitter norms, Sens. Actuators B 2005, 111, 286–292.

21. C. Caucheteur, M. Debliquy, D. Lahem, P. Megret, Catalytic fiber bragg grating sensor for hydrogen leak detection in air, IEEE Photonics Technol. Lett. 2008, 20, 96–98.

22. M. Krawczyk, J. Namiesnik, Application of a catalytic combustion sensor (Pellistor) for the monitoring of the explosiveness of a hydrogen–air mixture in the upper explosive limit range, Journal of Automated Methods & Management in Chemistry Vol. 25, No. 5, 2003, pp. 115–122.

23. M. Tong, J. Li, Y. Huang, X. Dai, Effect of electric field to catalytic sensor, IEEE International Conference on Information Acquisition, Weihai, China, August 2006, pp. 1005–1009.

24. P. Tardy, J. R. Coulon, C. Lucat, F. Menil, Dynamic thermal conductivity sensor for gas detection, Sens. Actuators B, 2004, 98, 63–68.

25. K. H. Kim, Performance characterization of the GC/PFPD for H2S, $CH_3SH$, $CH_3SCH_3$, and $CH_3SSCH_3$ in air, Atmos. Environ. 2005, 39, 2235–2242.

26. L. J. J. Catalan, V. Liang, C. Q. Jia, Comparison of various detection limit estimates for volatile sulphur compounds by gas chromatography with pulsed flame photometric detection, J. Chromatogr. A, 2006, 1136, pp. 89–98.

27. L. W. Schmerr, S. J. Song, Ultrasonic Nondestructive Evaluation Systems: Models and Measurements, Springer, New York, NY, USA, 2007.

28. G. Hallewell, G. Crawford, D. Mcshurley, G. Oxoby, R. Reif, A sonar based technique for the ratiometric determination of binary gas mixtures. Nucl. Instrum, Methods Phys. 1988, 264, pp. 219–234.

29. M. Shan, X. Li, C. Zhu, J. Zhang, Gas concentration detection using ultrasonic based on wireless sensor networks, ICISE, Hangzhou, China, 2010, pp. 2101–2106.

30. M. Sonoyama, Y. Kato, H. Fujita, Application of ultrasonic to a hydrogen sensor, IEEE Sensors, USA, November 2010, pp. 2141–2144.

31. S. Jacobson, New developments in ultrasonic gas analysis and flowmetering, IEEE International Ultrasonics Symposium, Beijing, China, 2–5 November 2008, pp. 508–516.

32. M. Sakai, S. Torii, Apparatus and Method for Measuring Gas Concentration, Japanese Patent JP2004325297, 18 November 2004.

33. R. H. Hammond, Ultrasonic Measurement System with Molecular Weight Determination, U.S. Patent 6,216,091, April 2001.

34. L. W. Schmerr, S. J. Song, Ultrasonic Nondestructive Evaluation Systems: Models and Measurements, Springer, New York, NY, USA, 2007.

35. Mylvaganam, S.; Halstensen, M.; Engen, H.; Esbensen, K. Gas density metering in ultrasonic gas flowmeters using impedance measurement and chemometrics. In Proceedings of 1999 IEEE Ultrasonics Symposium, Caesars Tahoe, NV, USA, 17–20 October 1999; pp. 435–439.

36. M. K. Sofian, M. E. Oussama, A. A. Imad, C. K. Marsha, Semiconducting metal oxide based sensors for selective gas pollutant detection, Sensors 2009, 9, pp. 8158–8196.

37. C. Wang, L. Yin, L. Zhang, D. Xiang, R. Gao, Metal oxide gas sensors: Sensitivity and influencing factors, Sensors 2010, 10, pp. 2088–2106.

38. A. Wisitsoraat, Tuantranont, E. Comini, Sberveglieri, W. Wlodarski, Characterization of n-type and p-type semiconductor gas sensors based on $NiO_x$ doped $TiO_2$ thin films, Thin Solid Films 2009, 517, pp. 2775–2780.

39. N. Yamazoe, K. Shimanoe, Theory of power laws for semiconductor gas sensors, Sens. Actuators B, 2002, 128, pp. 566–573.

40. M. Batzill, U. Diebold, The surface and materials science of tin oxide, Prog. Surf. Sci. 2005, 79, pp. 47–154.

41. H. Hallil, F. Chebila, P. Menini, P. Pons, H. Aubert, Feasibility of wireless gas detection with an FMCW RADAR interrogation of passive RF gas sensor, IEEE Sensors, Kona, USA, November 2010, pp. 759–762.

42. L. Fraiwan, K. Lweesy, A. Bani-Salma, N. Mani, A wireless home safety gas leakage detection system, MECBME, United Arab Emirates, February 2011, pp. 11–14.

43. K. Jarmo, M. Jani, H. Niina, K. Teemu, T. Géza, S. Maria, S. Andrey, M. Jyri-Pekka, J. Heli, K. Krisztián, Gas sensors based on anodic tungsten oxide, Sens. Actuators B 2011, 153, pp. 293–300.

44. T. A Emadi, C. Shafai, M. S. Freund, D. J. Thomson, D. S. Jayasz, N. D, G. Whitex, Development of a polymer-based gas sensor-humidity and $CO_2$ sensitivity, MNRC, Ottawa, Canada, October 2009, pp. 112–115.

45. H. Yoon, Current Trends in Sensors Based on Conducting Polymer Nanomaterials, Nanomaterials, 2013, 3, pp. 524-549, https://doi.org/10.3390/nano3030524.

46. A. G. Shrivas, R. G. Bavane, A. M. Mahajan, Electronic nose: A toxic gas sensor by polyaniline thin flim conducting polymer, IWPSD 2007, Mumbai, India, Dec 2007, pp. 621-623.

47. J. V. Hatfid, P. Neaves, P. J. Hicks, K. Persaud, P. Travers, Sens. Actuator B, 18, 1994, pp. 221-228.

48. L. Yang, Z. Rongwei, D. Staiculescu, C. P. Wong, M. M. Tentzeris, IEEEAntennas wirel, Propag. Lett. 8, 2009, pp. 653-656.

49. H. Bai, G. Shi, Gas sensors based on conducting polymers, Sensors, 7, 2007, pp. 267–307.

50. C. Hagleitner, D. Lange, A. Hierlemann, O. Brand, H. Baltes, CMOS single-chip gas detection system comprising capacitive, calorimetric and mass-sensitive microsensors, IEEE J. Solid-St. Circ. 2002, 37, pp. 1867–1878.

51. A. Modi, N. Koratkar, E. Lass, B. Wei, P. M. Ajayan, Miniaturized gas ionization sensors using carbon nanotubes, Nature, Vol. 424, 2003, pp. 171-174.

52. A. Mehdipour, I. Rosca, A. Sebak, C. W. Trueman, S. V. Hoa, Advanced carbon-fiber composite materials for RFID tag antenna applications, Appl. Comput. Electrom. J, 2010, 25, pp. 218–229.

53. G. O. Keat, Z. Kefeng, C. A. Grimes, A wireless, passive carbon nanotube-based gas sensor, IEEE Sens. J, 2, 2002, pp. 82–88.

54. J. K. Seong, The effect on the gas selectivity of CNT-based gas sensors by binder inSWNT/silane sol solutions IEEE Sens, Journal 10, 2010, pp. 173-177.

55. Y. Liu, M. Chen, M. Mohebbi, M. L. Wang, M. R. Dokmeci, The effect of sequence length on DNA decorated CNT gas sensors, ISSS, Actutors and Microsystems Conference, Beijing, Chaina, June 2011, pp. 2156-2159.

56. A. Wisitsoraat, A. Tuantranont, E. Comini, G. Sberveglieri, Gas sensing properties of CNT-$SnO_2$ nanocomposite thin film prepared by E-beam evaporation, IEEE Sensors, Atlanta, USA, Oct 2007, pp. 550-553.

57. F. Schedin, A. K. Geim, S. V. Morozov, E. W. Hill, P. Blake, M. I. Katesnelson, K. S. Novoselov, Detection of Individual Gas Molecules Adsorbed on Graphene, Nat. Mater 6, 2007, pp. 652-655, http://dx.doi.org/10.1038/nmat1967.

58. G. O. Keat, Z. Kefeng, C. A. Grimes, A wireless, passive carbon nanotube-based gas sensor, IEEE Sens. J, 2, 2002, pp. 82–88.

59. S. Johan, Z. Xuezhi, T. Unander, A. Koptyug, H. Nilsson, Remote moisture sensing utilizing ordinary RFID tags. IEEE Sensors, Atlanta, USA, Oct 2007, pp. 308-311.

60. T. Radadiya, A Properties of Graphene, European Journal of Material Science, Vol 2, No. 1, Sept 2015, pp. 6-18.

61. M. Kaur, P. K. Tripathi, The basic properties of Graphene and its applications, IJRAR, Volume 5, Issue 4, ISSN 2349-5138, December 2018, pp. 937-944.

62. A. Modi, N. Koratkar, E. Lass, B. Wei, P. M. Ajayan, Miniaturized gas ionization sensors using carbon nanotubes, Nature, Vol. 424, 2003, pp. 171-174.

63. A. T. Smith, A. M. LaChance, S. Zeng, B. Liu, L. Sun, Synthesis, properties, and application of grapheme oxide/ reduced grapheme oxide and their nanocomposites, Nano Materials Science, Vol. 1, 2019, pp. 31-47.

64. S. Preziose, L. Ottaviano, Graphene oxide: From fundamentals to applications, Journal of Physics Condensed Matter, 2015, pp. 1-21. doi:10.1088/0953-8984/27/1/013002.

65. S. I. Abdullah, M. N. M. Ansari, Mechanical properties of grapheme oxide (GO)/ epoxy composites, HBRC Journal, ISSN: 1687-4048, 2015, pp. 151-156. Doi:10.1016/j.hbrcj.2014.06.001.

66. J. G. S. Moo, B. Khezri, R. D. Webster, M. Pumera, Graphene Oxide Prepared by Hummers', Hofmann's, and Studenmair's Methods: Dramatic Influences on Heavy-Metal-Ion Adsorption, European Chemistry Societies Publishing, 2014, pp. 2922-2929.

67. H. L. Poh, F. Sanek, A. Ambrosi, G. Zhao, Z. Sofer, M. Pumera, Graphenes prepared by Staudenmair, Hofmann and Humers methods with

consequent thermal exfoliation exhibit very different electrochemical properties, Nanoscale 4, Royal Society of Chemistry, 2012, pp. 3515-3522.

68. V. O. Kotsyunky, V. M. Boychuk, I. M. Budzulyak, B. I. Rachiy, M. A. Hodlevska, A. I. Kachmar, M. A. Hodlevsky, Grapgene oxide synthesis using modified Tour method, IOP Science, Adv. Nat. Sci: Nanosci. Nanotechnol, Volume 12, doi 10.1088/2043-6262/ac204f.

69. A. Jirickova, O. Jankovsky, Z. Sofer, D. Sedmidubsky, Synthesis and Applications of Graphene Oxide, MDPI, Materials, 2022, 15, 920, pp. 1-21.

70. Q. A. Khan, A. Shaur, T. A. Khan, Y. F. Joya, M. S. Awan, L. N. Suvarupa, Characterization of reduced grapheme oxide produced through a modified Hoffman method, Cogent Chemistry 3, 2017, pp. 1-9.

71. O. Jankovsky, P. Marvan, M. Novacek, J. Luxa, V. Mazanek, K. Klimova, D. Sedmidubsky, Z. Sofer, Synthesis procedure and type of graphite oxide strongly influence resulting graphene properties, Applied Materials Today 4, 2016, pp. 45-53.

72. W. S. Hummers, R. E. Offeman, Preparation of Graphene Oxide, 1958, pp. 1339.

73. D. C. Marcsno, D. V. Kosynkin, J. M. Berlin, A. Sinitskii, Z. Sun, A. Slesarev, L. B. Alemany, W. Lu, J. M. Tour, Improved synthesis of graphene oxide, ACS Nano 2010, 4, 8, pp. 4806-4814. http://doi.org/10.1021/nm1006368.

74. B. Paulchamy, G. Arthi, B. D. Lignesh, A Simple Approach to Stepwise Synthesis of Graphene Oxide Nanomaterial, Journal of J Nanomedicine & Nanotechnology, ISSN: 2157-7439, Volume 6, pp. 1-4.

75. N. I. Zaabaa , K. L. Fooa, U. Hashima, S. J. Tanb, W. W. Liua, C.H. Voon, Graphene Oxide using Modified Hummers Method: Solvent Influence, Procedia Engineering 184, 2017, pp. 469–477.

76. M. Kaur, H. Kaur, D. Kukkar, Synthesis and characterization of graphene oxide using modified Hummer’s method, AIP Conference Proceedings 1953, 2018, 030180 (1-4), doi: 10.1063/1.5032515.

77. H. Yu, B. Zhang, C. Bulin, R. Li, R. Xing, High-efficient Synthesis of Graphene Oxide Based on Improved Hummers Method, Scientific Reports, 2016, pp. 1-7.

78. M. R. Karim, K. Hatakeyama, T. Matsui, H. Takehira, T. Taniguchi, M. Koinuma, Y.Matsumoto, T. Akutagawa, T. Nakamura, S. Noro, T. Yamada, H. Kitagawa, S. Hayami,Graphene oxide nanosheet with high proton conductivity, J. Am.Chem. Soc. 135(2013) pp. 8097–8100.

79. K. Hatakeyama, M. R. Karim, C. Ogata, H. Tateishi, A. Funatsu, T. Taniguchi, M. Koinuma,S.Hayami, Y. Matsumoto, raphene oxide nanosheets: single, Proton Conductivities of Graphene Oxide Nanosheets: Single, Multilayer, and Modified Nanosheets, A journal of the German Chemical Society, 2014, pp. 1-5. https://doi.org/10.1002/anie.201309931.

80. L. Guo, H. B. Jiang, R. Q. Shao, Y. L. Zhang, S. Y. Xie, J. N. Wang, X. B. Li, F. Jiang, Q. D. Chen, T. Zhang, H. B. Sun, Two-beam-laser interference mediated reduction, patterning and nanostructuring of graphene oxide for the production of a flexible humidity sensing device, Carbon 50, 2012, pp. 1667–1673.

81. I. Jung, D. Dikin, S. Park, W. Cai, S.L. Mielke, R.S. Ruoff, Effect of water vapor onelectrical properties of individual reduced graphene oxide sheets, J. Phys. Chem. C 112, 2008, pp. 20264–20268.

82. M. G. Chung, D. H. Kim, H. M. Lee, T. Kim, J. H. Choi, D. K. Seo, J. B. Yoo, S. H. Hong, T. J. Kang, Y. H. Kim, Highly sensitive $NO_2$ gas sensor based on ozone treated graphene, Sens. Actuators B, 2012, pp. 172–176.

83. X. Li, W. Cai, J. An, S. Kim, J. Nah, D. Yang, R. Piner, A. Velamakanni, I. Jung, E. Tutuc,S.K. Banerjee, L. Colombo, R.S. Ruoff, Large-area synthesis of high-quality and uniformgraphene films on copper foils, Science 324, 2009, pp. 1312–1314.

84. G. Lee, B. Lee, J. Kim, K. Cho, Ozone adsorption on graphene: an initio study andexperimental validation, J. Phys. Chem. C 113, 2009, pp. 14225-14229.

85. J. T. Robinson, F. K. Perkins, E. S. Snow, Z. Wei, P. E. Sheehan, Reduced graphene oxidemolecular sensors, Nano Lett. 8, 2008, pp. 3137–3140.

86. W. I. Yim, X. G. Gong, Z. F. Liu, Chemisorption of $NO_2$ on carbon nanotubes, J. Phys.Chem. B 107, 2003, pp. 9363–9369.

87. S. Prezioso, F. Perrozzi, L. Giancaterini, C. Cantalini, E. Treossi, V. Palermo, M. Nardone,S. Santucci, L. Ottaviano, Graphene oxide as practical solution to high sensitivity gassensing, J. Phys. Chem. C 117, 2013, pp. 10683–10690.

88. E. Treossi, M. Melucci, A. Liscio, M. Gazzano, P. Samori, V. Palermo, High contrastvisualization of graphene oxide on dye sensitized glass quartz, and silicon by fluorescence quenching, J. Am. Chem. Soc. 131, 2009, pp. 15576–15577.

89. E. Treossi, M. Melucci, A. Liscio, M. Gazzano, P. Samori, V. Palermo, High contrast visualization of graphene oxide on dye sensitized glass quartz, and silicon by fluorescence quenching, J. Am. Chem. Soc. 131, 2009, pp. 15576–15577.

90. S. Liu, B. Yu, H. Zhang, T. Fei, T. Zhang, Enhancing $NO_2$ gas sensing performances at room temperature based on reduced graphene oxide-ZnO nanoparticles hybrids, Sens. Actuators B 202, 2014, pp. 272–278.

91. S. Cui, H. Pu, E. C. Mattson, Z. Wen, J. Chang, Y. Hou, C.J. Hirschmugl, J. Chen, Ultrasensitive chemical sensing through facile tuning defects and functional groups in reduced graphene oxide, Anal. Chem. 86, 2014, pp. 7516–7522.

92. W. Li, X. Geng, Y. Guo, J. Rong, Y. Gong, L. Wu, X. Zhang, P. Li, J. Xu, G. Cheng, M. Sun, L. Liu, Reduced graphene oxide electrically contacted

graphene sensor for highly sensitive nitric oxide detection, ACS Nano 5, 2011, pp. 6955–6961.

93. G. Lu, S. Park, K. Yu, R.S. Ruoff, L.E. Ocola, D. Rosenmann, J. Chen, Toward practical gas sensing with highly reduced graphene oxide: A new signal processing method to circumvent run-to-run and device-to-device variations, ACS Nano 5, 2011, pp. 1154–1164.

94. S. Hwang, J. Lim, H.G. Park, W.K. Kim, D. H. Kim, I. S. Song, J. H. Kim, S. Lee, D. H. Woo, S. J. Chan, Chemical vapor sensing properties of graphene based on geometrical evaluation, Current Appl. Phys. 12, 2012, pp. 1017–1022.

95. N. Chen, X. Li, X. Wang, J. Yu, J. Wang, Z. Tang, S.A. Akbar, Enhanced room temperature sensing of $Co_3O_4$-intercalated reduced graphene oxide based gas sensors, Sens. Actuators B 188, 2013, pp. 902–908.

96. R. Arsat, M. Breedon, M. Shafiei, P.G. Spizziri, S. Gilje, R.B. Kaner, K. Kalantar-zadeh, W. Wlodarski, Graphene-like nano-sheets for surface acoustic wave gas sensor applications, Chem. Phys. Lett. 467, 2009, pp. 344–347.

97. A. Esfandiar, S. Ghasemi, A. Irajizad, O. Akhavan, M.R. Gholami, The decoration of TiO2/reduced graphene oxide by Pd and Pt nanoparticles for hydrogen gas sensing, Inter. J. Hydrogen Energy 37, 2012, pp. 15423–15432.

98. A. Esfandiar, A. Irajizad, O. Akhavan, S. Ghasemi, M.R. Gholami, Pd-WO3/reduced graphene oxide hierarchical nanostructures as efficient hydrogen gas sensors, International Journal of Hydrogen Energy, 2014, pp. 8169-8179.

99. P. A. Pandey, N. R. Wilson, J. A. Covington, Pd-doped reduced graphene oxide sensing films for $H_2$ detection, Sens. Actuators B 183, 2013, pp. 478–487.

100. Y. Du, Q. Xue, Z. Zhang, F. Xia, Great enhancement in $H_2$ response using graphene-based Schottky junction, Mater. Lett. 135, 2014, pp. 151–153.

101. T. Pustelny, S. Drewniak, M. Setkiewicz, E. Maciak, M. Urbanczyk, M. Procek, K. Gut, Z. Opilski, J. Jagiello, L. Lipinska, The sensitivity of sensor structures with oxide graphene exposed to selected gaseous atmospheres, Bull. Pol. Acad. Sci. 61, 2013, pp. 705–710.

102. J. Wang, B. Singh, J. H. Park, S. Rathi, I. Y. Lee, S. Maeng, H. I. Joh, C. H. Lee, G. H. Kim, Dielectrophoresis of graphene oxide nanostructures by hydrogen gas sensor at room temperature, Sens. Actuators B 194, 2014, pp. 296–302.

103. S.-J. Choi, B.-H. Jang, S.-J. Lee, B.K. Min, A. Rothschild, I.-D. Kim, Selective detection of acetone and hydrogen sulfide for the diagnosis of diabetes and halitosis using $SnO_2$ nanofibers functionalized with reduced graphene oxide nanosheets, Appl. Mater. Interfaces 6, 2014, pp. 2588–2597.

104. Y. Hasegawa, A. L. Spetz, D. Puglisi, Ethylene Gas Sensor for Evaluating Postharvest Ripening of Fruit, IEEE- GCCE 2017, 978-1-5090-4045-2.

105. K. Das, B. Jana, M. Pramanik, M. Mallick, J. Das, J. Sengupta, Chemically synthesized ZnO nanocrystal-based ethylene sensor operative at natural humid condition, Applied Physics A, 2022, pp. 1-6. https://doi.org/10.1007/s00339-022-06110-x.

106. L. P. Wang, Z. Jin, T. Luo, Y. Ding, J. H. Liub, X. F. Wang, M. Q. Li, The detection of ethylene using porous ZnO nanosheets: Utility in determination of Fruit Ripeness, The Royal Society of Chemistry, 2022, pp. 1-8.

107. M. Barth, T.R. Hankinson, H. Zhuang, F. Breidt, Microbiological Spoilage of Fruits and Vegetables, Springer Science + Business Media, 2009, pp. 135-183.

108. A. B. Bleecker, H. Kende, Ethylene: A Gaseous Signal Molecule is Plants, Annu. Rev. Cell Dev. Biol, 2000, pp. 1-18.

109. M. E. Saltveit, Effect of ethylene on quality of fresh fruits and vagetables, Postharvest Biology and Technology 15, 1999, pp. 279-292.

110. S. P. Burg, E. A. Burg, Role of Ethylene in fruits Ripening, Amarican Society of Plant Biologist, 1962, pp. 179-188.

111. M. S. Reid, M. J. C. Rhodes, A. C. Hulme, Changein Ethylene and $CO_2$ During the Ripening of Apples, J. Sci. Fd Agric, 1973, pp. 971-979.

112. S. M. Cristescu, J. Mandon, D. Arslanov, J. D. Pessemier, C. Hermans, F. J. M. Harren, Current methods for detecting ethylene in plants, Annals of Botany 111, 2013, pp. 347-360.

113. D. C. Dumitras, D. C. Dutu, C. Matei, A. M. Magureanu, M. Petrus, C. Popa, M. Patachia, Measurement of Ethylene Concentration by Laser Photoacoustic Techniques with Applications at Breath Analysis, Romanian Reports in Physics, Vol.-60, 2008, pp. 593-602.

# Chapter 2

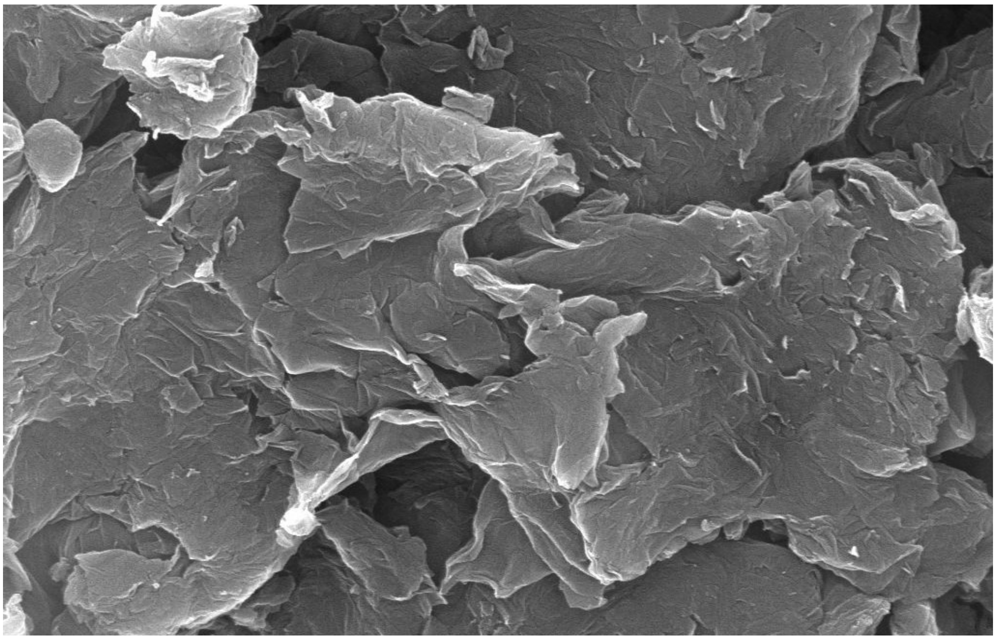

# *Chapter 2*

# Development of Graphene Oxide (GO) based Ethylene Sensor

## 2.1 Introduction:

The oxidized version of graphene is known as graphene oxide (GO). GO, a single atomic layered, ultrathin two-dimensional $sp^3$ hybridized honey-comb material [1,2], also known as graphitic oxide or graphitic acid, a compound of carbon, oxygen, and hydrogen in different ratios, is a popular sensor material that helps to detect various gases (like Acetylene ($C_2H_2$) [3], Ammonia ($NH_3$) [4], Nitrogen dioxide ($NO_2$) [5], etc.).

GO sheets have been used to produce robust membranes, thin films, composite materials, and paper-like materials [6, 7]. Initially, GO has attracted a lot of attention as a potential middleman in the synthesis of graphene. Numerous chemical and structural imperfections remain in the graphene created by reducing GO, which may be helpful in some applications but troublesome in others [6].

GO is prepared by very easily oxidation of inexpensive, widely accessible graphite. It has excellent physical properties and large specific surface area like Graphene [8], and has a unique sensor response due to irregular structure and surface absorbates [9]. -For this reason, we have used it as gas sensing material. The added advantage of GO is that it disperses in water and other solvents very easily [10].

In this chapter, first we have prepared GO by Hummer's method [11-14], using fine graphite powder, $NaNO_3$ and $KMnO_4$. Then the prepared GO has been characterized structurally and morphologically by Field Emission Scanning Electron Microscope, X-ray Diffraction technique and Ramman Spectroscopy. Finally, using this GO, pellet sensor and drop casted thin film sensor have been fabricated.

## 2.2 Experimental:

### 2.2.1 Formation of GO using Hummer's Method:

Standard Hummer's method was used to prepare GO [11-14]. A glass container with 50 ml of $H_2SO_4$ (98%) solution was kept inside an ice bath maintaining temperature at around 0–10 °C. Then, 2 gm of $NaNO_3$ and 2 gm of pure Graphite Powder were mixed into the solution under continuous stirring.

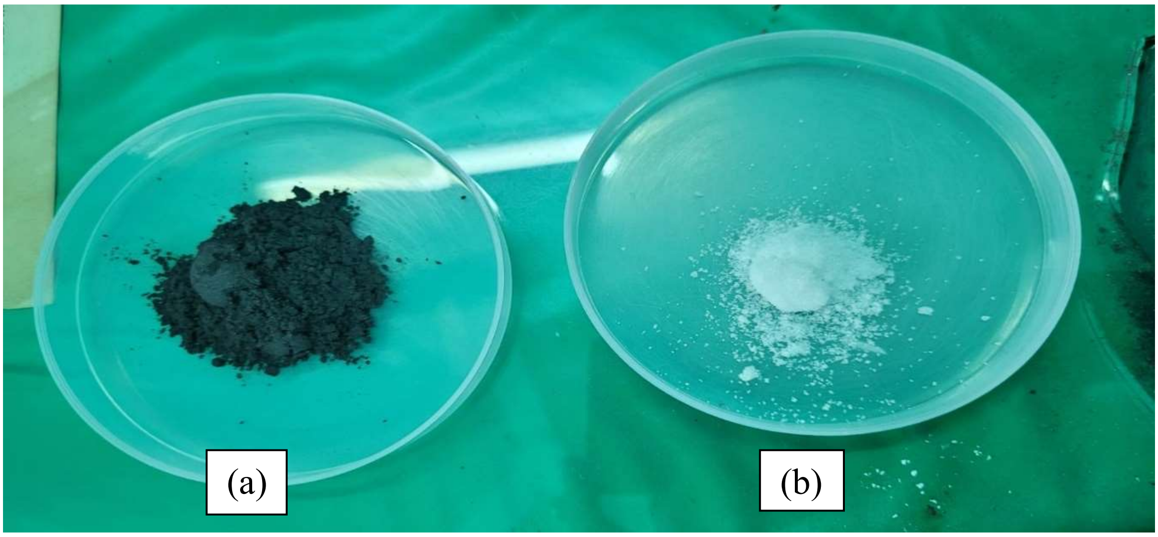

**Figure: 2.1** Photographs of (a) Pure Graphite Powder, (b) Sodium Nitrate

After 1 h stirring, 6 gm of $KMnO_4$ was added very slowly with carefully controlling the rate of addition to keep reaction temperature below 15 °C. After that, the ice bath was removed to let the solution temperature to increase up to 35 °C. The solution was further left under continuous stirring for another 2 h until formation of brownish precipitate completes. Then 100 ml of pure distilled water was added very slowly, and temperature was rapidly increased to 95 °C. Further, this solution was diluted by adding extra 200 ml of water with continuous stirring. Finally, to terminate the reaction, 10 ml of $H_2O_2$ was added to the brownish solution and color instantly changes to yellow. At room temperature, the solution was washed with 10% HCl and de-ionized (DI) water repeatedly until pH of the solution became 7. Finally, the precipitate was collected after filtration and dried at room temperature.

**Figure: 2.2** Pictures of borosil beaker under ice bath with continuous stirring.

### 2.2.2 Fabrication of GO sensors:

The dried precipitate was ground in a mortar and pestle before to obtain fine GO powder which was further used to prepare GO pellets. 400 mg quantity of powdered GO was pressed to form a 1 cm diameter pellet shown in Figure 2.3 (a).

To form thin film sensor, the collected precipitate was drop casted on a clear glass slit and dried at room temperature shown in Figure 2.3 (b).

On the pellets, two top electrodes were formed by coating Ag paste at room temperature.

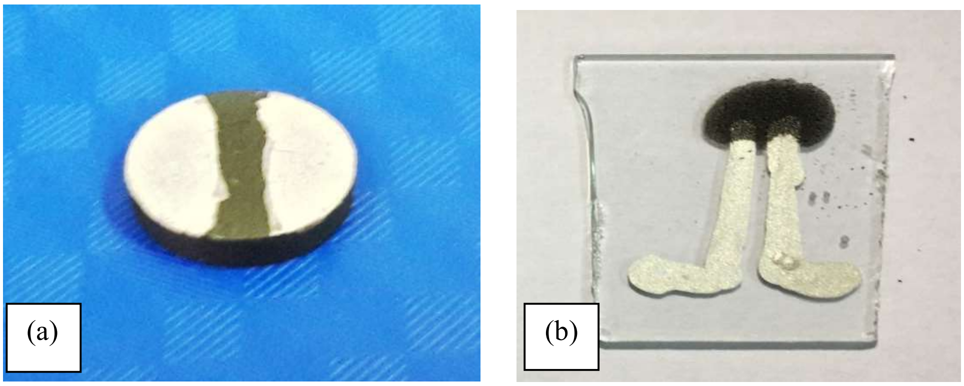

**Figure: 2.3** Photograph of (a) GO pellet sensor, (b) GO thin film sensor

### 2.2.3 Characterization:

Morphological characterization of the prepared multilayered GO was performed by field emission scanning electron microscope (FESEM) (JOEL, JSM-7610F), and structural characterization was performed by X-ray diffraction technique (Bruker D8 advance diffractometer) and Raman spectroscopy (J-Y Horiba confocal triple Raman spectrometer fitted with gratings of 1800 grooves/mm, Model: T64000).

## 2.3 Results and Discussions:

### 2.3.1 X-Ray Diffraction:

A nondestructive method known as X-Ray Diffraction analysis (XRD) can give precise details on a material's crystallographic structure, chemical makeup, and physical characteristics [15]. Its foundation is a crystalline sample with constructively interfering monochromatic X-rays.

The multilayered GO samples were characterized by X-ray powder diffraction having Cu Kα radiation of wavelength 1.5406 Å. Inside the scanning angle 2θ ~ range 5–85°, two distinct peaks were observed which were typical for multilayered GO structure. Figure: 2.4 shows diffraction peak at 2θ=10.65˚ corresponding to inter-planner spacing of 8.308 Å [16] and <002> plane of GO [17, 18]. Another peak at 2θ=42.39˚ was observed having d-spacing of 2.06 Å, corresponding to the <100> plane [18, 19] which might be generated due to the presence of oxygen-containing functional groups in graphene oxide and intercalated water molecules [20-25].

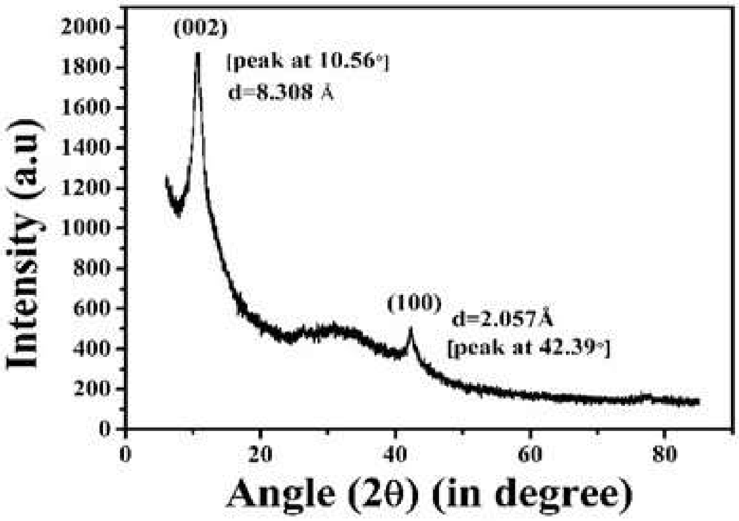

**Figure: 2.4** XRD pattern of prepared GO

### 2.3.2 FESEM:

With an essentially infinite depth of field, field emission scanning electron microscopy (FESEM) gives information on topography and elements at magnifications ranging from 10x to 300,000x. Despite having modest accelerating voltages and short working distances, it offers ultra-high resolution images [26].

Field FESEM micrograph of graphene oxide sample indicates the formation of ultrathin, homogeneous and multilayered graphene oxide sheets as shown in Figure: 2.5. It shows sheet like forms without any amorphous or other kind of crystallized phase of particles. The GO samples were observed to have flaky texture and layered microstructure [27-30].

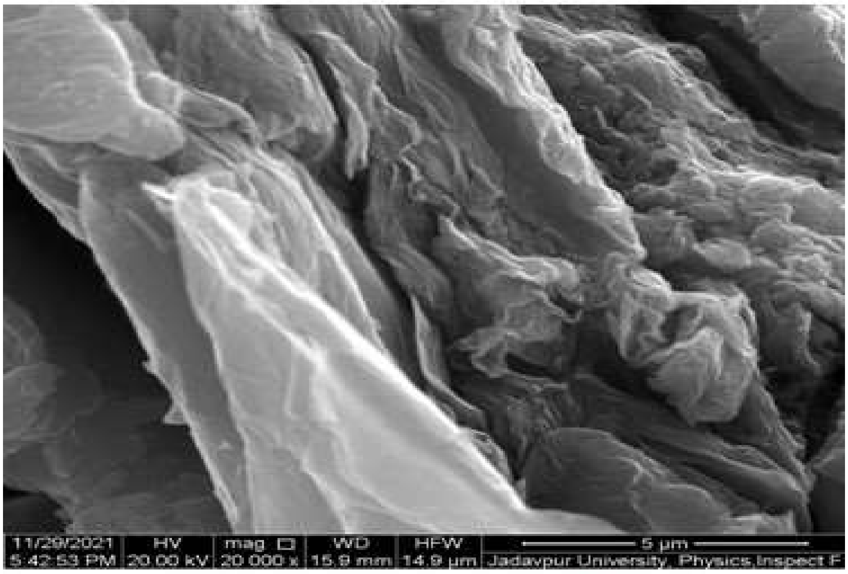

**Figure: 2.5** FESEM micrograph of GO

## 2.3.3 Raman Spectroscopy:

A non-destructive technique for chemical analysis, Raman spectroscopy provides comprehensive information on crystallinity, chemical structure, phase and polymorphy, and molecular interactions. It is based on how light interacts with chemical interactions in a substance [31].

The Raman spectra of the GO samples are shown in Figure: 2.6, which is used to determine the defects, the ordered and disordered structures in the sample. The two peaks, D peak at 1347 $cm^{-1}$ and G-peak at 1601 $cm^{-1}$ corresponding to the well-documented bands and the intensity ratio of D/G= 0.84 (>1), is due to the defects and partially disordered crystal structure of graphene [32-35]. It is clearly noticed that the intensity of D band is significantly higher than G band, suggesting that the prepared graphene has high defect content.

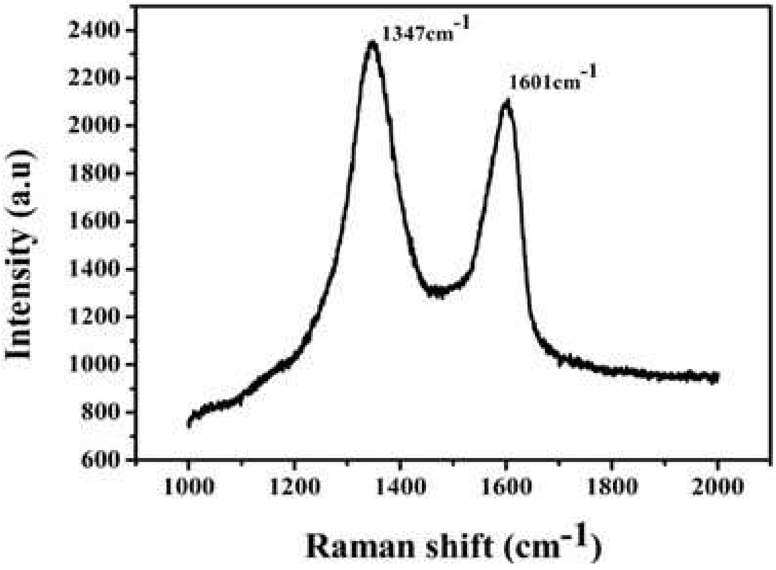

**Figure: 2.6** Raman spectra of GO

## 2.4 Conclusion:

Graphene oxide (GO) was prepared chemically using well known Hummer's method with the help of pure graphite powder, concentrated sulphuric acid ($H_2SO_4$, 98%), $KMnO_4$, sodium nitrate ($NaNO_3$) and then characterized structurally by X-Ray Diffraction (XRD), Field Emission Scanning Electron Microscope (FESEM) and Raman spectroscopy techniques.

After that, the prepared dried GO precipitate was grinded in mortar pestle before to obtain fine GO powder which was further used to prepare GO pellets. 400 mg quantity of powdered GO was pressed to form a 1cm diameter pellet. And another types of ethylene thin film sensor were prepared with the help of drop casted GO on a clear glass slit at room temperature. On the pellets two top electrodes were formed by coating Ag paste at room temperature. GO based conductive type ethylene gas sensor has been fabricated and tested using different fruits at room temperature.

Finally, our prepared graphene oxide-based Ethylene sensor show sensitivity, reliable, maximum change in resistance, stability, etc., all of these are discussed in next chapter.

## References:

1. F. Perrozzi, S. Prezioso, L. Ottavino, Graphene oxide: from fundamentals to applications, IOP Publishing, Journal of Physics: Condensed Matter, 27, 2015, pp. 1-21. doi:10.1088/0953-8984/27/1/013002.

2. L. Sun, Structure and synthesis of graphene oxide, Elsevier, Chinese Tournal of Chemical Enjineering 27, 2019, pp. 2251-2260.

3. A. S. M. LftekharUddin, D. T. Phan, G. S. Chung, Low temperature acetylene gas sensor based on Ag nanoparticles-loaded ZnO-reduced graphene oxide hybrid. Sensors and Actuators B: Chemical, Elsevier, 2015, pp. 362-369.

4. M. Yang, Y. Wang, D. Dong, Z. Xu, Y. Liu, N. Hu, E. Siu-Wai, J. Zhao, C. Peng, Gas Sensors Based on Chemically Reduced Holey Graphene Oxide Thin Films Yang et al. Nanoscale Research Letters, 2019, pp. 01-08. https://doi.org/10.1186/s11671-019-3060-5.

5. L. Guo, Y. W. Hao, P. L. Li, J. F. Song, R. Z. Yang, Z. Y. Fu, S. Y. Xie, J. Zhao, Y. L. Zhang,(2018) Improved NO2 Gas Sensing Properties of Graphene Oxide Reduced by Two-beam-laser Interference, SCIENTIFIC REPORTS, 2018, pp. 01-07, DOI:10.1038/s41598-018-23091-1.

6. A. N. Ghulam, O. A. L. dos Santos, L. Hazeem, B. P. Back, M. Bououdina, S. Bellucci, Graphene Oxide (GO) Materials—Applications and Toxicity on

Living Organisms and Environment, J. Funct. Biomater, 13, 77, 2022, pp. 1-28, https://doi.org/10.3390/jfb13020077.

7. A. T. Smith, A. M. LaChance, S. Zeng, B. Liu, L. Sun, Synthesis, properties, and applications of graphene oxide/reduced graphene oxide and their nanocomposites, Nano Materials Science 1, 2019, pp. 31–47.

8. K. Toda, R. Furue, S. Hayami, (2015) Recent progress in applications of graphene oxide for gas sensing: A review, Elsevier, Analytica Chimica Acta, Vol 878, 2015, pp. 43-53. https://doi.org/10.1016/j.aca.2015.02.002

9. A. Lipatov, A. Varezhnikov, P. Wilson, V. Sysoev, A. Kolmakov, A. Sinotskii, Highly selective gas sensor arrays based on a thermally reduced graphene oxide, RSC Publishing, Nanoscale, 2013, pp. 5426-5434.

10. R. T. M. Ahmad, S. Hong, T. Shen, J. Song, Water-assisted stable dispersal of graphene oxide in non-dispersible solvents and skin formation on the GO dispersion, Carbon 98, 2016, pp. 188-194, DOI:10.1016/j.carbon.2015.11.007.

11. B. Paulchamy, G. Arthi, B. D. Lignesh, A Simple Approach to Stepwise Synthesis of Graphene Oxide Nanomaterial, Journal of J Nanomedicine & Nanotechnology, ISSN: 2157-7439, Volume 6, pp. 1-4.

12. N. I. Zaabaa , K. L. Fooa, U. Hashima, S. J. Tanb, W. W. Liua, C.H. Voon, Graphene Oxide using Modified Hummers Method: Solvent Influence, Procedia Engineering 184, 2017, pp. 469–477.

13. M. Kaur, H. Kaur, D. Kukkar, Synthesis and characterization of graphene oxide using modified Hummer's method, AIP Conference Proceedings 1953, 2018, 030180 (1-4), doi: 10.1063/1.5032515.

14. H. Yu, B. Zhang, C. Bulin, R. Li, R. Xing, High-efficient Synthesis of Graphene Oxide Based on Improved Hummers Method, Scientific Reports, 2016, pp. 1-7.

15. A. Andrei, E. Gabriela, Y. Hassan, X - RAY DIFFRACTION: Instrumentation and Applications, Analytical Chemistry, 2015, pp. 1-38.

16. S. Drewnik, R. Muzyka, A. Stolarczyk, T Pustelny, M. Kotyczka-Mora, M. Setkiewicz, Studies of Reduced Graphene Oxide and Graphite Oxide in the Aspect of Their Possible Application in Gas Sensors, Sensor 2016, 2016, pp. 1-16.

17. S. Rana, S. Maddila, S. B. Jonnalagadda, Synthesis and characterization of Pd (II) dispersed over diamine functionalized graphene oxide and its scope as a catalyst for selective oxidation, Royal Society of Chemistry, 5, 2015, pp. 3235-3241.

18. Y. Sheng, X. Tang, E. Peng, J. Xue, Graphene oxide based fluorescent nanocomposites for cellular imaging, RSC Publishing, The Royal Society of Chemistry, 2013, pp. 512-521.

19. Y. Li, W. Gao, L. Ci, C. Wang, P. M. Ajayan, Catalytic performance of Pt nanoparticles on reduced graphene oxide for methanol electro-oxidation, Elsevier, Carbon 48, 2009, pp. 1124–1130, http://dx.doi.org/10.1016/j.carbon.2009 .11.034.

20. S. N. Alam, N. Sharma, L. Kumar, Synthesis of Graphene Oxide (GO) by Modified Hummers Method and Its Thermal Reduction to Obtain Reduced Graphene Oxide (rGO), Scientific Research Publishing, 2017, pp.01-18.

21. M. Mallick, J. Das, Graphene oxide based ethylene gas sensor for e-nose application, Invertis Journal of Science and technology, 10, 2017, pp.178-182.

22. S. Bykkam, V. K. Rao, S. C. CH, T. Thunugunta, SYNTHESIS AND CHARACTERIZATION OF GRAPHENE OXIDE AND ITS ANTIMICROBIAL ACTIVITY AGAINST Klebseilla AND Staphylococus, International Journal of Advanced Biotechnology and Research, 4, 2013, pp. 142-146.

23. L. Stobinski, B. Lesiak, B. Malolepszy, M. Mazurkiewicz, B. Mierzwa, J. Zemek, P. Jiricek, I. Bieloshapka, Graphene oxide and reduced graphene oxide studied by the XRD, TEM and electron spectroscopy methods, Elsevier, 2014, pp. 145-154. https://doi.org/10.1016/j.elspec.2014.07.003

24. M. Mallick, S. M. Hossain, J. Das, Graphene Oxide Based Fruit Ripeness Sensing e-Nose, Elsevier, Materials Today: Proceedings, 2018, pp. 9866-9870. https://doi.org/10.1016/j.matpr.2017.10.179

25. X. Wang, S. Nie, P. Zhangc, Y. Hua, Elsevier, Journal of materials research and technology, 2020, pp. 667-674.

26. B. Lewczuk, S. Natalia, Field-Emission Scanning Electron Microscope as a Tool for Large-Area and Large-Volume Ultrastructural Studies, MDPI, Animals 2021, 11, 3390, pp. 1-21.

27. S. N. Alam, N. Sharma, L. Kumar, Synthesis of Graphene Oxide (GO) by Modified Hummers Method and Its Thermal Reduction to Obtain Reduced Graphene Oxide (rGO), Scientific Research Publishing, 2017, pp. 01-18. **DOI:** 10.4236/graphene.2017.61001

28. M. Mallick, J. Das, Graphene oxide based ethylene gas sensor for e-nose application, Invertis Journal of Science and technology, 10, 2017, pp. 178-182.

29. L. Stobinski, B. Lesiak, B. Malolepszy, M. Mazurkiewicz, B. Mierzwa, J. Zemek, P. Jiricek, I. Bieloshapka, Graphene oxide and reduced graphene oxide studied by the XRD, TEM and electron spectroscopy methods, Elsevier, 2014, pp. 145-154.

30. M. Mallick, S. M. Hossain, J. Das, Graphene Oxide Based Fruit Ripeness Sensing e-Nose, Elsevier, Materials Today: Proceedings, 2018, pp. 9866-9870.

31. U. P. Agarwal, R. H. Atalla, Raman Spectroscopy, CRC Press, Inc.: 152-181, Chapter 8, 1995, pp. 152- 181. DOI:10.1007/978-3-642-74065-7_12.

32. V. Scardaci, G. Compagnini, Raman Spectroscopy Investigation of Graphene Oxide Reduction by Laser Scribing, Journal of Carbon Research, 2021, pp. 1- 7, https://doi.org/10.3390/c7020048

33. K. N. Kudin, B. Ozbas, H. C. Schniepp, R. Prud'homme, I. A. Aksay, R. Car, Raman Spectra of Graphite Oxide and Functionalized Graphene Sheets, American Chemical Society, Nano Letters, 8, 2018, pp. 36-41. https://doi.org/10.1021/nl071822y

34. A. Kaniyoor, S. Ramaprabhua, A Raman spectroscopic investigation of graphite oxide derived graphene, AIP Advance, 2, 2012, pp. 1-13. https://doi.org/10.1063/1.4756995.

35. W. Oh, F. Zhang, Preparation and Characterization of Graphene Oxide Reduced From a Mild Chemical Method, Asian Journal of Chemistry, 23, 2011, pp. 875-879.

# Chapter 3

# Chapter 3
# Fruit Freshness Sensor

## 3.1 Introduction:

Fruit freshness monitoring is an extremely crucial field in food industry for customer satisfaction and minimization of loss due to wastage [1, 2]. But freshness monitoring is not easy for large scale packaging and marketing industry just by human eye sorting. Every year, only in India, about 30% of produced fruits and vegetables are lost due to spoilage [3]. Ethylene ($C_2H_4$) is a colorless, tasteless, non-polar hydrocarbon [4] which is also a natural ripening (or aging) plant hormone that has numerous effects on the growth, development and storage life of many fruits [5-7].

In different stages of ripening, Ethylene is emitted from the fruits which can be monitored to detect perfect ripening conditions. Also, for different fruits under same ripening condition, the amount of emitted Ethylene can vary which may be utilized for identifying individual fruits in e-nose applications [8]. Several works on Ethylene based fruit ripeness monitoring have already been reported in the last few years [9]. State of the art processes for detection and monitoring of ethylene gas concentration are gas chromatography [10], electro-chemical sensing [11,12] or laser-based photo-acoustic spectroscopy [13,14] etc., most of which are very much expensive and difficult to use for on-field applications.

Graphene oxide can be defined as a single layer of $sp^3$ hybridized carbon atoms. These carbon atoms bear oxygen-containing functional groups on the basal and edge plane [15,16]. It is a widely used sensor material that has been used to detect a variety of gases, like Acetylene ($C_2H_2$) [17], Ammonia ($NH_3$) [18], Nitrogen dioxide ($NO_2$) [19] etc. Preparation of GO is easy and cost efficient and it has significantly large specific surface area like Graphene [20] and has a unique sensor response due to irregular structure and surface absorbates [21]. For all these advantages of GO, we have chosen it as core nanomaterials for ethylene gas sensing.

In this chapter, we have developed multilayer graphene oxide based conductive type Ethylene gas sensors, (a) pellet type and (b) drop casted thin film type to detect change in concentration of ethylene due to fruit ripening. The sensor has been kept in a closed chamber with four different fruits (like: Orange, Banana, Guava, Mango) of same mass (200gm) under same ripening condition separately. The same experiment has also been performed for a particular fruit (banana) at different ripening condition (i.e. unripe, ripe and over ripe). From the response characteristics, different sensor parameters like sensitivity, repeatability, reproducibility and storage stability have been observed. For fixed exposure time, different fruits produced different amount of output current which can be utilized for recognizing a particular fruit via GO based e-nose. Also, a particular fruit at different amount of output current indicating the presence of different amount of emitted ethylene. Sensing response of the drop casted thin film GO sensor has been compared with another two well known gas sensing materials ZnO and $MoS_2$. Temperature optimization and interference of ambient humidity have also been studied. Finally, a sensing mechanism has been proposed.

## 3.2 Experimental

### 3.2.1 Gas Sensing Setup

Figure: 3.1 shows a gas sensing setup developed in our laboratory for the sensing measurements. The resistance variation of the GO based sensors is recorded at room temperature in presence and absence of ethylene gas emitted from different fruits. A sample holder with a heating and cooling arrangement is placed inside the sensing chamber to study the optimized temperature for sensing.

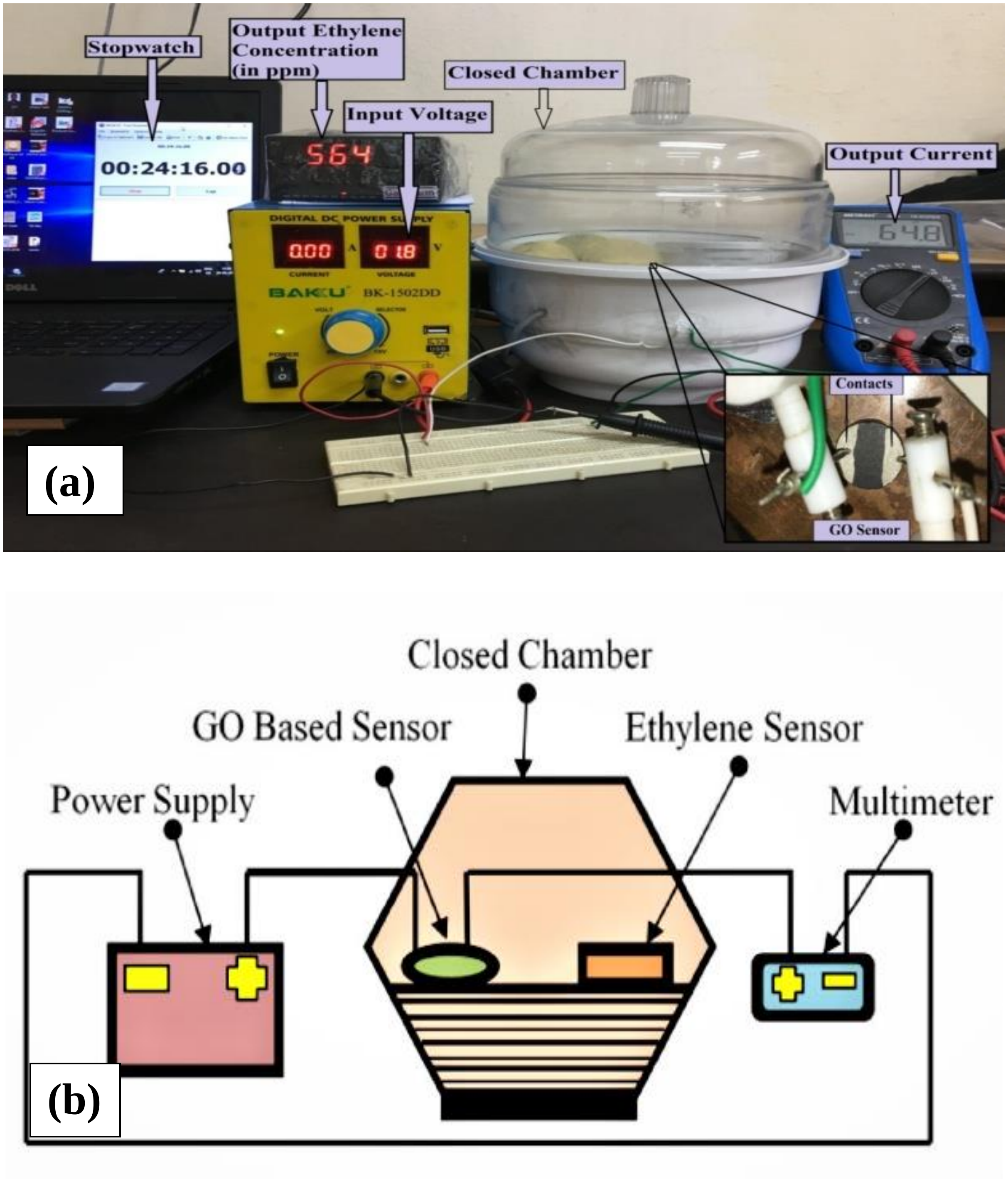

**Figure: 3.1** Gas sensing setup (a) actual photograph, (b) Schematic diagram.

### 3.2.2 Gas Sensor Measurements:

Sensing measurements of the prepared GO based sensor were performed using a gas sensing set up inside a vacuum desiccator (Figure: 3.1). A fixed voltage of 2V across the electrodes of the GO pellet was supplied. Transient-current response of the sensor was monitored for a fixed time interval in presence and absence of different fruits of same mass (200gm) at room temperature. The current response was recorded using multi-meter and Kiethley 2450 source meter. A commercially available Ethylene gas sensor (MSR Ethylene sensor, MA-3-2089-F-F) along with our developed GO based sensor was kept in the same closed chamber for calibration. Also, a humidity and temperature measuring sensor (Hygrometer testo 608-H1) was placed inside the sensing chamber for temperature optimization and to study the interference of humidity in gas sensor. First, any one type of fruit was placed inside the closed sensing chamber for five minutes and the transient current values were recorded. Corresponding $C_2H_4$ concentrations detected by MSR sensor have also been observed which provides a current vs. gas concentration calibration curve. After that, the chamber was opened and the fruit was taken out, and the sensor was allowed to reach the initial current value. This process was repeated for several times for each fruit.

## 3.3 Results and Discussions:

### 3.3.1 Response Study:

When the banana is placed inside the closed sensing chamber, $C_2H_4$ gas concentration inside the chamber increases with time and reaches a saturation value depending upon the emission rate of $C_2H_4$ from the fruit. The transient response of the sensor at 2V applied bias has been measured in presence of unripe, ripe and over ripe banana at room temperature (Figure: 3.2).

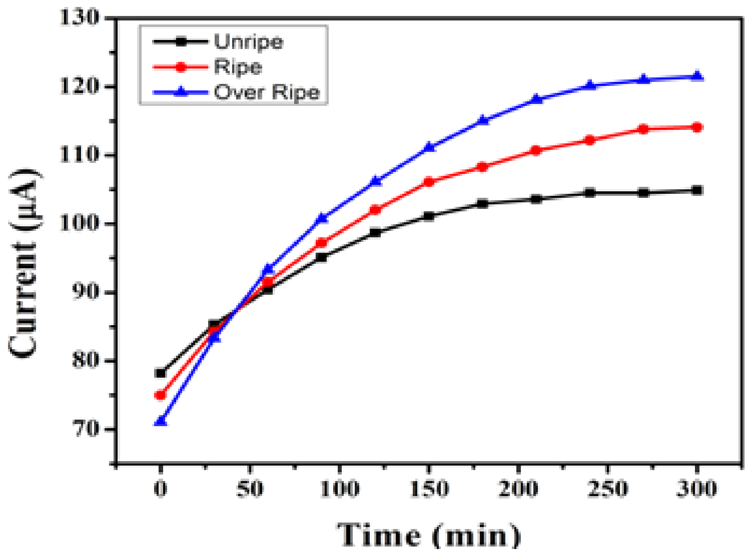

**Figure: 3.2** Transient- Current Response

Accordingly, the transient current value of the sensor increases with time and becomes saturated. Again, the emission rate of $C_2H_4$ depends on the degree of ripeness. The transient response curves give highest current values in case of over ripe fruit indicating highest $C_2H_4$ concentration compared to the unripe and ripe fruits. So, after proper calibration, from the transient response of our developed GO based sensor, the degree of ripeness of a particular fruit can be estimated [22].

Calibration curve of GO pellet sensor is plotted in Figure: 3.3 for fixed time interval of 5 minute. As the fruit placed inside the desiccator emits Ethylene gas, the concentration of Ethylene increases inside the enclosed chamber. Ethylene concentration was monitored using MSR sensor and corresponding current output of the GO pellet sensor was recorded. It was observed that after 5 minute exposure time, orange samples produced maximum amount of Ethylene corresponding to maximum output current while mango produced minimum output response. So, it is evident that for a fixed exposure time GO pellet sensor is capable to distinguish different fruits based upon the amount of Ethylene emitted by them. The sensitivity of Go pellet sensor was calculated from the linear fit of the response curve corresponding to orange samples which was found to be 0.06 µAmp/PPM. Standard MSR sensors have a system resolution of 20 PPM and it is impossible for them to detect ethylene concentration beyond this range. GO pellet sensor was found to have a system resolution much lower than MSR sensors (~ 5 PPM).

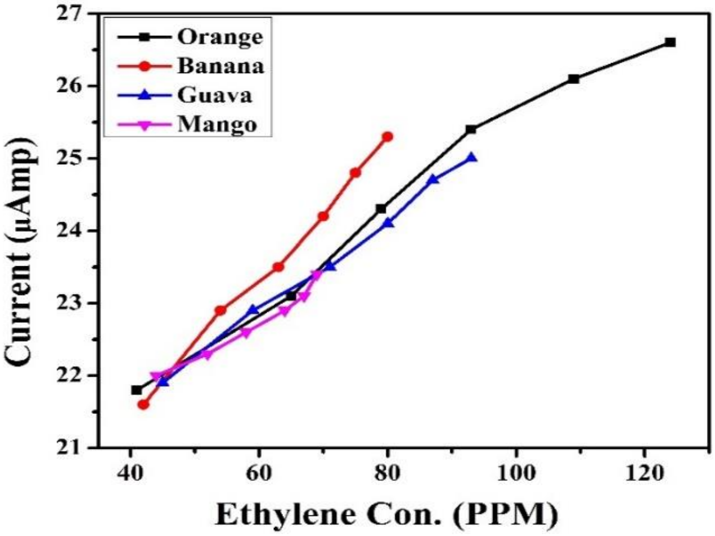

**Figure: 3.3** Calibration curve of GO pellet sensor (Fixed exposure time of 5minute and bias voltage of 2 volt)

The ethylene sensing performance of the GO sensor was studied by measuring the conductance change of the GO pellet in presence and absence of ethylene. The percentage change in resistance of the sensor on ethylene exposure is defined as,

$$\text{Response}(S) = \left[\frac{\text{R}_{\text{air}} - \text{R}_{\text{ethylene}}}{\text{R}_{\text{air}}}\right] \text{X } 100$$

The response of the sensor along with response time and desorption time when exposed to different fruits of same mass and in same ripening condition at room temperature are summarized in Table-1. These values differ significantly for different fruits.

**Table-1:** Summarized sensor parameters for different fruits.

| Fruits | Response (S) (%) | Maximum Change in Resistance (KΩ) | Desorption Time (Min) |
|---|---|---|---|
| 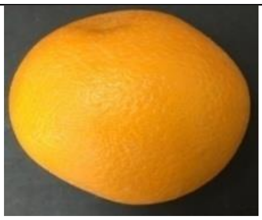<br>Orange | 18.0 | 16.473 | 1.56 |
| <br>Banana | 12.4 | 12.630 | 1.47 |
| <br>Guava | 10.3 | 11.454 | 1.37 |
| <br>Mango | 6.0 | 6.273 | 1.49 |

### 3.3.2 Repeatability study:

The repeatability study was performed for three cycles with all the four types of fruits. After 5-minute exposure time the chamber was opened and fruit sample was removed. It was observed that the sensor output current reached initial value after approximately 1.47 minute after opening the enclosed chamber. So, desorption time of the GO pellet sensor was found to be around 1.47 minute. Also, from the repeatability curve (Figure: 3.4) obtained from three consecutive cycles, it was observed that the sensor is quite suitable for repeated use.

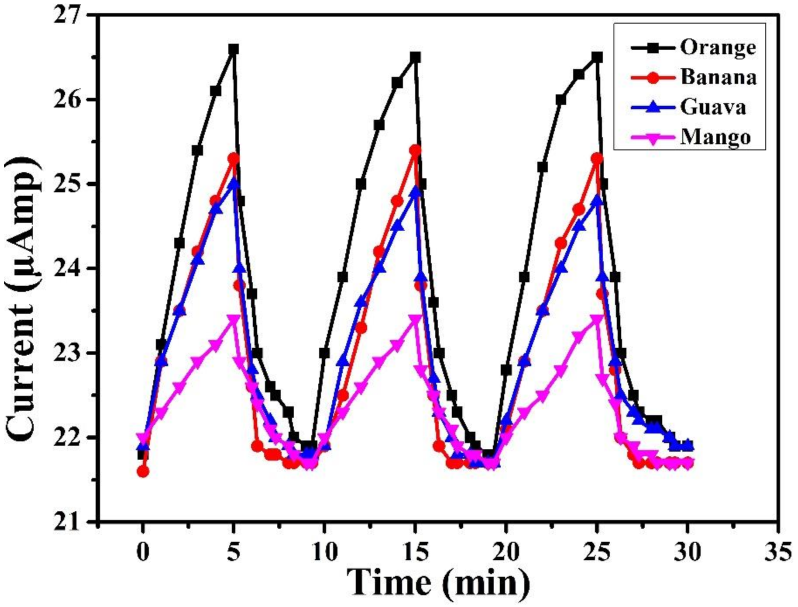

**Figure: 3.4** Repeatability curve of GO pellet sensor

### 3.3.3 Reproducibility Study:

Reproducibility of the GO pellet sensor was observed for three different pellets prepared under same condition in different time. Reproducibility of the sensor is depicted in Figure: 3.5 for four different fruits. For orange samples a mean value of 23.76 µAmp with a SD ±0.057 corresponding to 65 PPM was observed (n=3), except mango samples which produced SD as large as ±0.11. All the three pellets show good reproducibility.

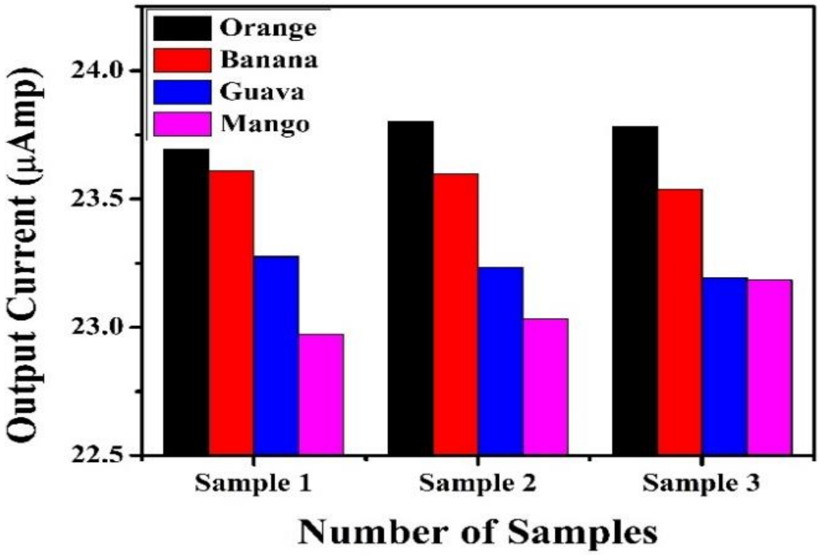

**Figure: 3.5** Reproducibility curve of GO pellet sensor

### 3.3.4 Storage Stability Study:

Storage stability of the GO pellet sensors was studied for 19 days at room temperature. First-day current reading ($I_1$) of the GO pellet sensor corresponding to 70 PPM $C_2H_4$ concentration has been used to normalize the dataset, and normalized current ($I/I_1$) was plotted against storage day in Figure: 3.6. It was observed that after 11th day, the response falls drastically and thus stability of the sensor is found to 10 days. To increase the sensor storage stability further studies are required to identify the reason behind degradation and to find out suitable solution of this drawback.

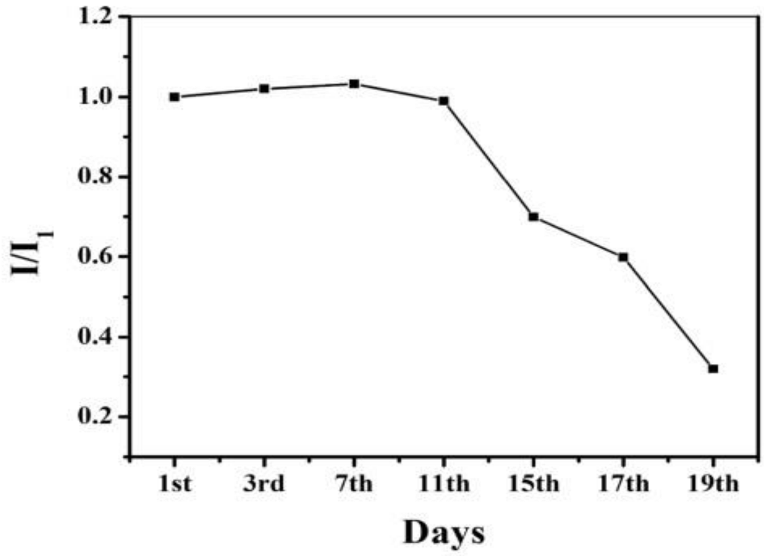

**Figure: 3.6** Storage stability of GO pellet sensor

### 3.3.5 Temperature Optimization:

To optimize the operating temperature, the drop casted GO based sensor device was tested at various temperatures ranging from 17 ºC to 42 ºC. Figure: 3.7, shows the response of our GO based ethylene sensor at different temperatures for ~50 ppm of ethylene gas concentration liberated from guava. The plot clearly shows that the sensor is most sensitive at temperature ~22ºC, which is close to our room temperature. The applied voltage between the electrodes was 2V.

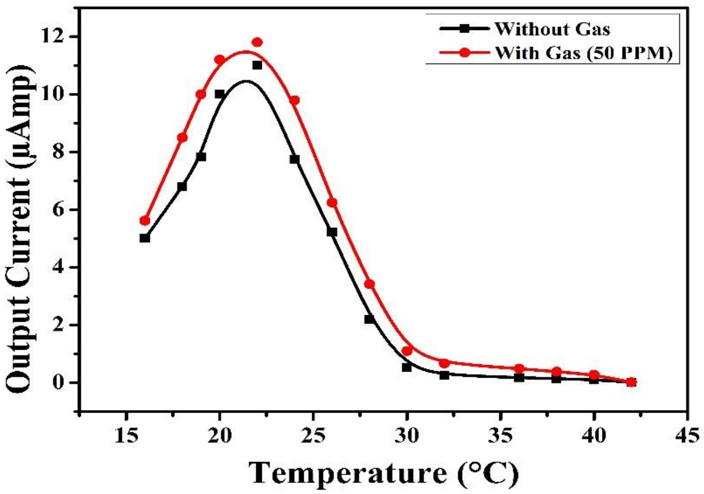

**Figure: 3.7** Temperature Optimization of GO sensor

## 3.3.6 Humidity Interference:

Finally, the interference of ambient humidity in ethylene gas sensing has also been studied. Like any other gas sensors, humidity is found to affect significantly the sensing measurements of our sensor. Figure: 3.8 shows the sensor response at 40 and 60 PPM ethylene concentration with relative humidity ranging from 55 to 95%. It is clear from the figure that the sensor response has increased on order of magnitude for the higher value relative humidity.

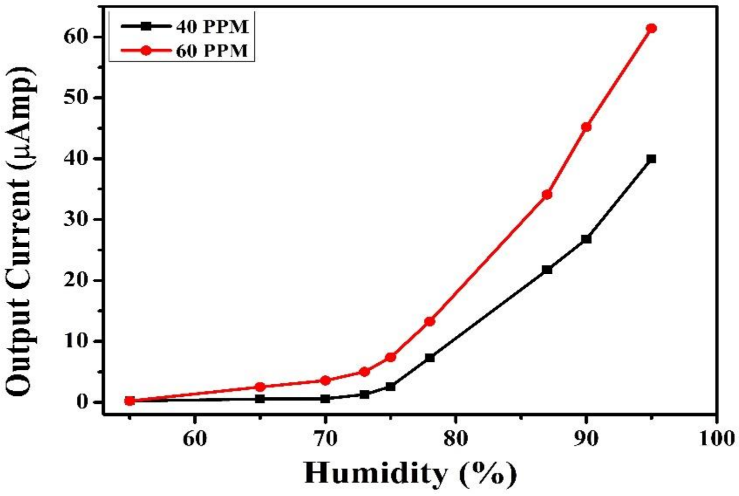

**Figure: 3.8** Humidity response study of GO sensor

### 3.3.7 Comparison with other materials:

We also compared the performance of our GO based sensor with other sensors made from two well-known sensing materials, ZnO and $MoS_2$. Here we use drop casted materials instead of pellet, which is shown in Figure: 3.9. At room temperature, a fixed bias voltage (2 Volts) was applied across the two electrodes of the sensor device and output current was recorded with a guava as the source of ethylene gas. The output current vs ethylene concentrations clearly identify that GO based Ethylene sensor is most impactful compared to the other two materials which is shown in Figure: 3.10.

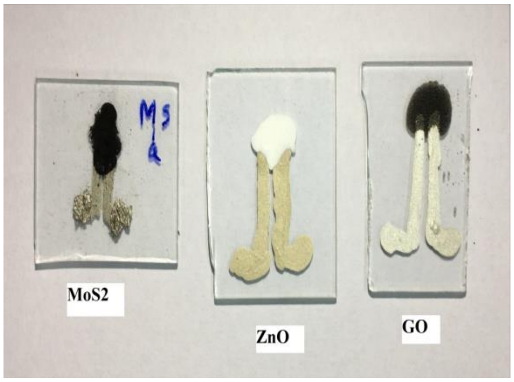

**Figure: 3.9** Drop casted materials in glass slit.

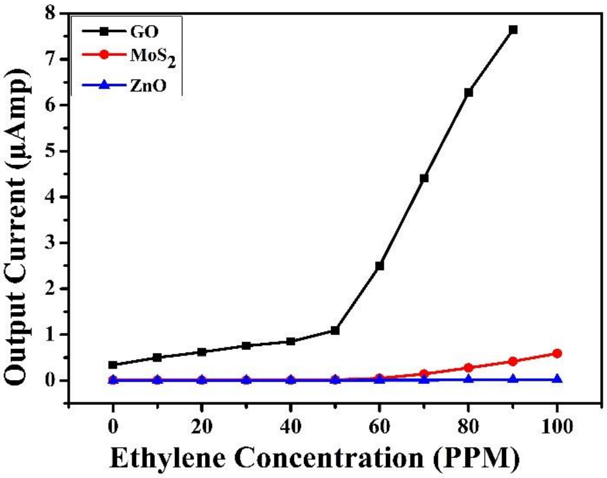

**Figure: 3.10** Comparison with another materials graph.

## 3.4 Sensing Mechanism:

In our GO based conductive type ethylene gas sensor, the conductivity of GO sensing layer increases with increasing ethylene concentration. Here, we propose a sensing mechanism. During oxidation of graphite, oxygen functional groups bond with carbon plane leading to numerous C-O bonds where electrons are pulled away from carbon atoms towards oxygen atoms producing holes in the carbon network [23-25].

Thus, GO shows p-type semiconductor behavior. Oxygen atoms on GO surface often form non-stoichiometric bonds [26] which are a key factor behind the gas sensing mechanism of GO pallets.

Ethylene is a reducing gas [27] which reacts with these non-stoichiometrically attached oxygen atoms present on GO surface leaving behind surface holes which increases carrier concentration in p-type GO pallet. So, with increase in ethylene concentration more and more surface holes are generated leading to constant increase in the conductivity of the samples.

## 3.5 Conclusion:

In the previous chapter, we have discussed the fabrication of GO based conductive type ethylene gas sensors for freshness monitoring of fruits. In this chapter, the sensors have been tested using different fruits at room temperature in a closed sensing chamber specially designed by the purpose.

The sensor can clearly identify different fruits having the same mass in perfect ripening condition, thus can be used to differentiate between different ripe fruits in e-nose application. For a particular fruit, the sensor can also differentiate the unripe, ripe and over ripe condition. GO pellet sensors show sensitive and reliable ethylene gas-sensing performance. The sensor shows the capability of lower resolution from standard MSR sensors with good reproducibility.

The comparative study of response clearly shows that our GO based sensor is more sensitive towards ethylene compared to other well known gas sensing materials. Finally, a sensing mechanism has been proposed to understand the conductive type sensing of GO based ethylene gas sensor.

# References:

1. M. Sarkar, N. Gupta, M. Assaad, Monitoring of fruit freshness using phase information in polarization reflectance spectroscopy, Optical Society of America, 58, 2019, pp. 6396-6405.

2. A. U. Alim, P. Rathi, H. Beshai, G. K. Sarabha, M. J. Deen, Fruit Quality Monitoring with Smart Packaging, MDPI, Sensors, 21, 2021, pp. 1-30.

3. S. Rawat, Asian J. Plant Sci. Res, Food Spoilage: Microorganisms and their prevention, 2015, pp. 47-56.

4. A. Sahgal, H. M. La, W. Hayduk, Solubility of ethylene in several polar and non-polar solvents, The Canadian Journal of Chemical Engineering, 1978, pp. 354-357.

5. N. Keller, M. N. Ducamp, D. Robert, V. Keller, Ethylene Removal and Fresh Product Storage: A Challenge at the Frontiers of Chemistry. Toward an Approach by Photocatalytic Oxidation, ACS Publications, 2013, pp. 5029-5070.

6. N. Iqbal, N. A. Khan, A. Ferrante, A. Trivellini, A. Francini, M. I. R. Khan, Ethylene Role in Plant Growth, Development and Senescence: Interaction with Other Phytohormones, Frontiers in Plant Science, 2017, pp. 1-19.

7. M. E. Saltveit, Effect of ethylene on quality of fresh fruits and vegetables, Elsevier, 1999, pp. 279-292.

8. M. Baietto, A. D. Wilson, Electronic-Nose Applications for Fruit Identification, Ripeness and Quality Grading, Sensors 2015, 15, 899-931; doi:10.3390/s150100899.

9. S. Janssen, K. Schmitt, M. Blanke, M. L. Bauersfeld, J. Wollenstein, W. Lang, Ethylene detection in fruit supply chains, Royal Society Publishing, 2022, pp. 1-21.

10. N. A. Zaidi, M. W. Tahir, P. P. Vinayaka, F. Lucklum, M.Vellekoop, W. Lang, Detection of Ethylene Using Gas Chromatographic System, Elsevier, Procedia Engineering 168, 2016, pp. 380-383.

11. J. F. M. Oudenhoven, M. A. G. Zevenbergen, W. Knoben, R. V. Schaijk, Electrochemical Ethylene Sensor for Fruit Monitoring Based On An Ionic Liquid Electrolyte, 224th ESC Meeting 2013.

12. S. Janssen, K. Schmitt, M. Blanke, M. L. Bauersfeld, J. Wollenstein, W. Lang, Ethylene detection in fruit supply chains, Royal Society Publishing, 2014, pp. 01-21.

13. M. Cristescu, J. Mandon, D. Arslanov, J. M. D. Pessemier, C. Hermans, F. J.

M. Harren, F. J. M. Oxford University Press, 2012, pp. 01-14.

14. C. Popa, Ethylene Measurements from Sweet Fruits Flowers Using Photoacoustic Spectroscopy, MDPI, Molecules, 24, 2019, pp. 1144.

15. F. Perrozzi, S. Prezioso, L. Ottavino, Graphene oxide: From fundamentals to applications, Journal of Physics: Condensed Matter, 27, 2015, pp. 1-21.

16. L. Sun, Structure and Synthesis of graphene oxide, Elsevier, Chinese Tournal of Chemical Enjineering 27, 2019, pp. 2251-2260.

17. A. S. M. LftekharUddin, D. T. Phan, G. S. Chung, Low temperature acetylene gas sensor based on Ag nanoparticles-loaded ZnO-reduced graphene oxide hybrid, Sensors and Actuators B: Chemical, Elsevier, 2015, pp. 362-369.

18. M. Yang, Y. Wang, D. Dong, Z. Xu, Y. Liu, N. Hu, E. Siu-Wai, J. Zhao, C. Peng, Ammonia gas sensors based on chemically reduced graphene oxide sheets self-assembled on Au electrodes, Nanoscale Research Letters, 2019, pp. 01-08.

19. L. Guo, Y. W. Hao, P. L. Li, J. F. Song, R. Z. Yang, Z. Y. Fu, S. Y. Xie, J. Zhao, Y. L. Zhang, Improved $NO_2$ Gas Sensing Properties of Graphene Oxide Reduced by Two-beam-laser Interference, SCIENTIFIC REPORTS,

2018, pp. 01-07.

20. K. Toda, R. Furue, S. Hayami, Recent progress in applications of graphene oxide for gas sensing: A review, Elsevier, Analytica Chimica Acta, 878, 2015, pp. 43-53.

21. A. Lipatov, A. Varezhnikov, P. Wilson, V. Sysoev, A. Kolmakov, A. Sinotskii, Highly selective gas sensor arrays based on thermally reduced graphene oxide, RSC Publishing, Nanoscale, 2013, pp. 5426-5434.

22. M. Mallick, J. Das, Graphene oxide based ethylene gas sensor for e-nose application, Invertis Journal of Science and Technology, Vol. 10, No. 4, 2017 ; pp. 178-182 DOI No.: 10.5958/2454-762X.2017.00029.4.

23. Y. F. Sun, S. B. Liu, F. Li. Meng, J. Y. Liu, Z. Jin, L. T. Kong, J. H. Liu, Metal Oxide Nanostructures and Their Gas Sensing Properties: A Review, Sensors 2012, pp. 2610-2631, https://doi.org/10.3390/s120302610.

24. Y. Xing, H. Zhu, G. Chang, K. Yu, F. Yue, MDPI, Sensors, 2019, pp. 1-8.

25. Y. Murashima, M. R. Karim, R. Furue, T. Matsui, H. Takehira, K. Wakata, K. Toda, R. Ohtani, M. Nakamura, S. Hayami, Reduced graphene oxide–transition metal hybrids as p-type semiconductors for acetaldehyde sensing, Royal Society of Chemistry, 2016, pp. 1-6.

26. D. R. Dreyer, S. Park, C. W. Bielawski, R. S. Ruoff, The chemistry of graphene oxide, The Royal Society of Chemistry, 2010, pp. 228-240.

27. J. Kathirvelan, R. Vijayaraghavan, A. Thomas, Ethylene detection using TiO2–WO3 composite sensor for fruit ripening applications, Sensor Review, 37, 2017, pp. 147-154.

# Chapter 4

# *Chapter 4:*

# Summary and Conclusions

## 4.1 Summary of the present work:

Graphene oxide (GO) is a viable platform for gas sensors due to its extremely high surface to volume ratio, the most crucial factor for improved gas adsorption, the first step in gas sensing. As GO is readily available and simple to prepare, it is also very simple to manufacture sensors utilizing it. GO as a gas sensor has certain limitations for commercial use despite its many benefits. The electrical response may be impacted by fermi level pinning caused by the high density of surface states. The research reported in this thesis sought to determine the potential of graphene oxide as a transducing material for fruit freshness monitoring application through ethylene ($C_2H_4$) gas sensing.

In the first chapter, an extensive literature survey is provided to understand the basic sensing mechanism of different types of gas sensors, their design methodology, choice of suitable substrates, device characterization and modelling. Based on this knowledge, the objective of the present thesis has been formulated. The main objective of the present work is to develop a GO based conductive type ethylene gas sensor for the freshness monitoring of fruits.

The second chapter deals with the fabrication and characterization of GO. GO has been prepared using Hummer's Method. The structural and morphological characterization of the prepared multilayered GO was performed by X-Ray Diffraction, Field Emission Electron Microscopy (FESEM) and Ramman Spectroscopy. After that, the powdered GO was pressed to form a pellet. Also, GO solution was drop casted on glass substrate to form thin film. On both the pellet and thin film sensors top electrodes were formed by coating room temperature Ag paste.

In chapter three, we have studied a multilayer graphene oxide based conductive type Ethylene gas sensor to detect change in concentration of ethylene due to fruit ripening. Here, the sensors have been tested using different fruits at room temperature in a closed sensing chamber specially designed by the purpose.

The sensor can clearly identify different fruits having the same mass in perfect ripening condition, thus can be used to differentiate between different ripe fruits in e-nose application. For a particular fruit, the sensor can also differentiate the unripe,

ripe and over ripe condition. GO pellet sensors show sensitive and reliable ethylene gas-sensing performance. The sensor shows the capability of lower resolution from standard MSR sensors with good reproducibility.

The comparative study of response clearly shows that our GO based sensor is more sensitive towards ethylene compared to other well known gas sensing materials. Finally, a sensing mechanism has been proposed to understand the conductive type sensing of GO based ethylene gas sensor.

## 4.2 Scope of Further Work:

The work reported in this thesis has led to some understanding of the enhanced sensitivity, selectivity and other parameters of the graphene oxide based conductive types ethylene gas sensors. Long term stability is an important factor for device application. Based on the limitations of the sensor system, further work can be initiated to improve the technology and sensing materials of the system for better performance. We have tested that GO is much more sensitive towards ethylene when compared to other hydro carbon has not been tested. This knowledge base will be utilized to carry out further studies in the following areas:

1. There are immense scope of further improvement of our sensing chamber, which affect our work significantly.
2. Use of better measuring instrument instead of multimeter and 100% closed chamber may increase the cost but reduce system noise significantly.

3. The integration of the sensor with commercially available radio frequency identification device (RFID) tags for in-field wireless monitoring of the ripening condition of fruits may be the future scope of work.